PB-226 961

URBAN INDUCED INFLUENCE ON CONVECTIVE CLOUD ACTIVITY

R. Paul Lawson

Wyoming University

Prepared for:

Environmental Protection Agency

March 1973

DISTRIBUTED BY:

NTIS

National Technical Information Service
U. S. DEPARTMENT OF COMMERCE
5285 Port Royal Road, Springfield Va. 22151

030105

PB 226 961

URBAN INDUCED INFLUENCE ON CONVECTIVE CLOUD ACTIVITY

R. PAUL LAWSON

REPORT No. AR107

Research Supported by the
Environmental Protection Agency,
Grant R-800875 (June 1, 1970)

MARCH 1973

Reproduced by
NATIONAL TECHNICAL
INFORMATION SERVICE
U S Department of Commerce
Springfield VA 22151

DEPARTMENT OF
ATMOSPHERIC
RESOURCES

College of Engineering
University of Wyoming , Laramie

60

URBAN-INDUCED INFLUENCES ON CONVECTIVE CLOUD ACTIVITY

by

R. Paul Lawson

Department of Atmospheric Resources
University of Wyoming
Laramie, Wyoming

December, 1972

PREFACE

This report contains the slightly revised text of a thesis prepared by Mr. R. Paul Lawson in partial fulfillment of the requirements for the Master of Science Degree in Atmospheric Resources.

Project METROMEX, the cooperative program between federal, state, university and private research groups, has been undertaken to examine the problem of inadvertent weather modification by an urban-industrial complex. The project represents a broad, multi-disciplined approach to the problem. Initial field studies were begun in St. Louis during the summer of 1971 with the University of Wyoming personnel conducting a one-month field program during the month of August.

The research described by Mr. Lawson examines urban-induced influences on daytime air mass convective cloud activity. In particular, these influences included two (or a combination of both) mechanisms whereby the potential mixing layer depth could be reduced, thus inhibiting convective cloud genesis and growth. Perhaps Mr. Lawson has not conclusively proved, or disproved, the effects of stabilizing the atmosphere by (a) entrainment of air from above the well-mixed layer and (b) radiated heating of aerosol layers; however, he has built a suitable argument implying that these mechanisms may be active. His work certainly demonstrates that further research in these areas must be expanded.

Finally, Mr. Lawson should be complimented on his diligent pursuit of data and literature review for this elusive research topic; it is such diligent pursuit that contributes the firm foundation of the better scientific researcher.

August H. Auer, Jr.

ABSTRACT

Three case study days (9, 13 and 23 August 1971) of Project METROMEX were selected on the merit of available data to investigate possible urban-induced influences on convective cloud activity. Data included observations from meteorologically equipped aircraft and mobile units, radiosondes and pilot balloons, lidar, surface temperature and dew point recording network, radar and 35-mm photographs.

Analyses of the data revealed regions where convective cloud activity was inhibited by the presence of an elevated thermally stable layer, while simultaneously, other regions showed cumulus development. Using a dimensional similitude analysis of a fluidal model, it was found that the atmospheric system may be capable of exhibiting elevated warming via turbulent entrainment of warm air downward through the elevated stable layer. Aerosol heating was also considered as a mechanism which may produce elevated heating.

Subsequent daytime elevated warming at and immediately beneath the elevated stable layer was found to shrink the potential mixing layer depth, inhibiting convective cloud activity. This relationship between mixing layer depth and convective cloud activity is consistent with other Project METROMEX synoptic analyses for dry summers.

TABLE OF CONTENTS

		Page
I.	INTRODUCTION	1
	1.1 The Role of Project METROMEX	1
	1.2 Inadvertent Weather Modification	1
	1.3 Statement of the Problem	1
II.	LITERATURE REVIEW	1
	2.1 The Modification of Convective Clouds by an Urban Area	1
	2.2 Urban Influences on Precipitation	1
	2.3 Urban Influences on Temperature	2
	Surface Temperature Investigations	2
	Vertical Temperature Profile Investigations	3
	Elevated Thermally Stable Layers	3
	Thermal Effects of Aerosol Layers	3
	2.4 Urban Influences on Moisture	4
	2.5 Urban Influences on Airflow	4
	2.6 Urban Influences on Turbulence	4
III.	EXPERIMENTAL DATA AND PROCEDURES	4
	3.1 General Description of St. Louis in Relation to Project METROMEX	4
	3.2 Explanation of Data Presentation	5
	3.3 Surface Data	6
	3.4 Aircraft Data	6
	3.5 Radiosonde and Wind Data	7
	3.6 Radar Data	7
	3.7 Lidar Data	7
IV.	DESCRIPTIVE ANALYSES OF RESEARCH RESULTS	7
	4.1 Research Approach	7
	4.2 23 August 1971 Case Study	7
	Synoptic Conditions	7
	Cloud Coverage	7
	Analysis of Convective Cloud Activity	11
	4.3 13 August 1971 Case Study	14
	Synoptic Conditions	14
	Cloud Coverage	15
	Analysis of Convective Cloud Activity	15
	4.4 9 August 1971 Case Study	15
	Synoptic Conditions	15
	Cloud Coverage	15
	Analysis of Convective Cloud Activity	15
	4.5 Composite Analysis of Convective Cloud Activity	15
V.	MECHANISTIC ANALYSIS OF RESEARCH RESULTS	17
	5.1 The Approach	17
	5.2 23 August 1971 Case Study	17
	Elevated Heating Profiles	17
	Advection in the Vicinity of an Elevated Stable Layer	19
	Vertical Transport of Air through an Elevated Stable Layer	23
	Radiative Effects of Aerosol Layers on Vertical Temperature Structure	33

Page

5.3 13 August 1971 Cast Study. 41
Elevated Heating Profile 41
Advection in the Vicinity of an Elevated Stable Layer. . 42
Examination of the Processes Associated with Elevated Heating 42
5.4 9 August 1971 Case Study 44
5.5 Moisture Distribution in the Three Case Study Days . . . 44
5.6 Climatological Implications. 45

VI. SUMMARY AND CONCLUSIONS 45

6.1 General Considerations 45
6.2 Regions of Preferential Convective Activity in the St. Louis Area 46
6.3 Urban Influences on Vertical Temperature Structure . . . 46
6.4 Mechanisms Associated with the Formation of Elevated Stable Layers and Elevated Heating 46

REFERENCES. 47

APPENDIX A. 52

APPENDIX B. 53

I. INTRODUCTION

1.1 The Role of Project METROMEX

Project METROMEX 1971 (METROpolitan Meteorological EXperiment) is a cooperative effort of researchers from Argonne National Laboratory, the University of Chicago, Illinois State Water Survey and the University of Wyoming. The overall objective of the Project is to statistically and physically evaluate the possible effects of the modification of weather and climate by an urban-industrial complex. St. Louis, Missouri was selected as the site for the Project.

1.2 Inadvertent Weather Modification

Since the time of the Industrial Revolution the world's population has been migrating toward urban centers. In western countries about 70 percent of the population lives in or near towns and cities and projections predict that 85 percent will live there by the year 2000 (Landsberg, 1970). The concept that an urban area may be capable of modifying weather in its vicinity has led to the coining of the term "inadvertent weather modification," i.e., consideration of an urban area as a potential weather modifier on the basis of its existence, as opposed to man's deliberate attempts to modify weather such as cloud seeding with silver iodide.

Although statistical analyses are crucial to the detection and evaluation of inadvertent weather modification, evaluation and understanding of the physical parameters involved is also necessary in order to lend credence to these statistics.

1.3 Statement of the Problem

Among the many meteorological and climatological parameters which may be affected by the influence of an urban-industrial complex, the study of the factors influencing the modification of convective cloud activity is one of the more arduous. One must consider spatial and vertical distributions of temperatures, moisture, wind, turbulence, the composition of the atmosphere, and effectively assess their respective contributions.

In recent climatological investigations of the St. Louis area, Beebe and Morgan (1972) and Huff and Changnon (1972) found that the St. Louis precipitation anomaly is chiefly associated with summer, convective, daytime, air mass rain storms. In light of this finding, and the fact that August 1971 was the fifth driest month on record in St. Louis (Changnon, 1971), this report will focus upon urban-induced influences on daytime air mass convective cloud activity. It is felt that an investigation of this type will help establish a physical foundation for the explanation of urban precipitation anomalies.

II. LITERATURE REVIEW

2.1 The Modification of Convective Clouds by an Urban Area

Until Project METROMEX, there was no direct field research conducted on the subject of urban influences on convective cloud activity. The only studies of an associated nature were conducted by Ackinson (1970, 1971). Two case studies of thunderstorms over the London area were examined utilizing recorded radar and surface network data. Using climatological data from the period 1951-1960, Atkinson (1968, 1969) determined that a statistically significant maximum of thunderstorm rainfall over central London was attributed to about ten summer storms out of 600. In one case, Atkinson concluded that a thunderstorm which developed in light winds showed that clouds initiated and precipitated over London's urban area, and that the initiation was due to local urban maxima of potential and wet-bulb potential temperatures. In the second case study, he concluded that a traveling thunderstorm passing over London was enhanced by the urban area as documented by an increase in radar tops and surface precipitation. This situation was again attributed to warm moist air in the urban area.

Of a secondary nature to this section, in the sense that no meteorological parameters were documented, are the observations of preferential cumulus formation over industrial complexes by Hoddinott (1960) and Stout (1962). Stout observed the selective formation of cumulus over a petro-chemical plant in central Illinois on five different occasions, while Hoddinott reported incidences of cumulonimbus downwind of the industrial complex at Chester, England.

2.2 Urban Influences on Precipitation

Since documented research into the area of urban influences on convective cloud activity is virtually non-existent, an investigation of the literature relative to the salient features of urban area precipitation studies contingent only to summer investigations serves to highlight the following features:

1. Urban areas generally record more precipitation then their surrounding rural vicinities in summer months. [However, in dry summers, Huff and Changnon (1972) have found evidence

that the St. Louis area may produce an urban-induced suppression effect on precipitation.]

2. The summer urban increase is more pronounced on weekdays as compared to weekends.

However, these generalizations must be put into perspective. Analyses which depend upon only two or three discrete recording sites to represent a selected area may not be wholly representative of urban-rural precipitation distributions. This consideration is elucidated in the works of Woolum and Canfield (1968), and the St. Louis study of Huff and Changnon (1972), where a network of precipitation gauges was utilized. Woolum and Canfield found the urban center in Washington, D. C. to represent a precipitation low when compared to its immediate surrounding area. In a recent consideration of Changnon's St. Louis data, Huff et al. (1971) compiled the average summer rainfall analysis shown in Figure 2.1. Notice that the precipitation highs are located northwest and east of the major urban buildup, while the city itself represents a relative precipitation low. As a consequence, one must be consistent in his definitions of "urban" and "rural" before assigning characteristic urban-rural differentials.

2.3 Urban Influences on Temperature

The heat island (or thermal island) is a term which has been defined as an area, generally around the center of urban buildup, where the average temperature is higher than that of the surroundings (American Meteorological Society, 1968). Various investigations (Malkus, 1955, 1957; Black, 1962; Atkinson, 1968, 1971) have suggested that heat islands may contribute to areas of preferential convective cloud formation. Findings of this type imply that an urban heat island may influence convective cloud activity.

Surface Temperature Investigations. Relatively little has been published on the daytime heat island effect. Landsberg (1956) has found that the heat island is often hard to distinguish in the daytime, and may even show a reverse effect in some cases. However, Landsberg points out that the data are quite erratic and that there are cases where the urban area has displayed higher temperature than its environs. Chandler (1965, 1966) has found that the annual average daytime maximum temperatures of London were 0.6 and 1.1C higher than those in surrounding areas. Munn et al. (1969) had no trouble distinguishing a daytime heat island during the time of maximum heating in Toronto, Canada. However, their data were complicated by the fact that rural stations

Reproduced from best available copy.

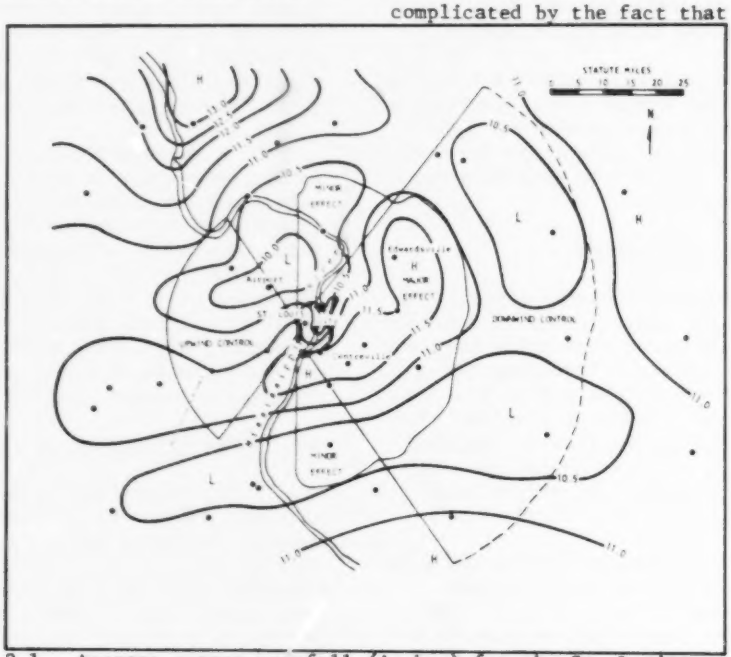

Figure 2.1. Average summer rainfall (inches) for the St. Louis area during the period 1949-1968 (After Huff et al., 1971).

were adjacent Lake Ontario and were frequently subject to the cooler on-shore sea-breeze. During the summer of 1967, Ludwig (1968) studied the daytime heat islands in Dallas and Fort Worth using horizontal time section analyses from mobile traverses over 24-hour periods. He found the maximum difference in urban-rural daytime temperatures to be about 1C. This maximum occurred in a ring around the cluster of tall buildings at the city's center where the temperature was 0.5C cooler than the ring maximum. Ludwig concluded that this cooler inner core seemed to be caused by the attenuation of solar radiation by the taller, larger buildings near the city's center.

Vertical Temperature Profile Investigations. In order to effectively assess an urban area's influence on convective cloud activity, a knowledge of the thermal structure below cloud base must be included.

Unfortunately, many urban area vertical temperature profile investigations (Duckworth and Sandberg, 1954; DeMarris, 1961; Pooler, 1963; Arnold, 1964; Munn and Stewart, 1967; Davidson, 1967; Bornstein, 1968; and Clarke, 1969) suffer three inadequacies when viewed in relation to convective cloud activity. First there is no documentation of the location of convective activity corresponding to vertical temperature structure. Second, vertical temperature profiles were terminated below 2500 ft AGL (with the exception of Davidson who showed profiles to 4200 ft AGL). Third, except for the instrumented tower observations and the work of Davidson (1967), experiments were conducted during early morning and/or late evening hours, suggesting that most of the inversions encountered were of the low-level radiational type. Therefore, very little work has been published on the vertical extent and magnitude of the summer daytime urban heat island.

Elevated Thermally Stable Layers. The presence of an elevated (1000-10,000 ft AGL) thermally stable layer (or temperature inversion) may significantly effect convective cloud activity. Of the previously mentioned urban area vertical temperature profile investigations, Davidson (1967) showed data of sufficient height to positively record the existence of elevated stable layers. Examination of Davidson's data for 1200 EST 9 March 1966 reveals elevated stable layers on all four soundings taken at that time in the New York area. These stable layers range from approximately 3000-3500 ft AGL and are all associated with a layer of adiabatic temperature lapse from the surface to the base of the stable layer. The strength of the stable layers is directly related to the decrease in SO_2 concentration upward through the vertical. Therefore, it was concluded that elevated stable layers existed at midday in the New York area on 9 March 1966, that their elevation was spatially dependent, and their relative strength was associated with the magnitude of vertical diffusion.

The presence of an elevated stable layer has also been documented by Olsson et al. (1971) in the Columbia-Willamette Valley region of Western Oregon. The results indicated that the "actual mixing height" as indicated by the top of the haze layer and strong reduction in aerosol concentrations, was closely correlated with stable layers aloft.

The work of Spangler (1972), in connection with Project METROMEX, has shown that elevated stable layers typically cap the mixing layer and that these layers are subject to spatial and time dependent altitude variations. On one of his two case study days (12 August 1971) Spangler found that the mixing layer "domed" the urban area, and that this doming was attributed to the lowering of the elevated stable layer outside the urban area between early morning and mid-afternoon.

Thermal Effects of Aerosol Layers. A somewhat recent consideration has been the effect of aerosol (haze) layers on the earth's heat budget. The theoretical investigations reported in the literature have been conflicting, but are usually a function of the parameters considered. For example, McCormick and Ludwig (1967) suggested that an increasing concentration of aerosols could increase the albedo and thus cool the earth. Charlson and Pilat (1969) reported that cooling or heating of the earth-atmosphere system depended upon the absorption-to-backscatter ratio of the aerosol. On the other hand, Schneider (1971) concluded that the effect of an aerosol is to reduce the total solar energy absorbed in the earth-atmosphere system, even if the aerosol absorption is comparable to its backscatter. In a reply, Charlson and Pilat (1971) stated that Schneider's model showed only "second order" differences due to the inclusion of the effects of multiple light reflections from the surface. Mitchell (1970) found that the effect of an aerosol may be warming or cooling depending on the absorption-to-backscattering ratio and the albedo of the underlying surface. He concluded that the predominant effect of tropospheric aerosol on the surface climate is one of warming, except in locally arid or urban regions where the effect would be marginal. Atwater (1970) suggested that the introduction of pollutants, particularly aerosols, into his numerical simulations for the urban environment caused

the development of elevated inversions (thermally stable layers). His results showed that radiative processes contribute to the formation of these elevated inversions.

It is apparent that the knowledgeable effects of aerosols are fragmentary at this time, but that the presence of aerosol layers indeed provides the capacity for augmentation of the earth's heat budget. Further theoretical and experimental investigations are necessary.

2.4 Urban Influences on Moisture

Reports of urban moisture distributions in the literature are, at best, infrequent and conflicting. It is generally agreed that the urban relative humidity is lower than surrounding rural areas; however, this may be attributable to the urban heat island effect. Some investigators have found the urban area to be slightly drier on an absolute scale during summer months (Kratzer, 1956; Landsberg, 1956, 1962; Chandler, 1962; Sasakura, 1965), others have seen a relatively higher urban absolute humidity (Chandler, 1967; Ackerman, 1971; Bornstein et al., 1972), while still others have seen no characteristic difference in moisture between summertime urban and rural air (Duckworth and Sandberg, 1954; Ludwig, 1968). In the two case studies considered by Atkinson (1970, 1971), he found relatively higher values of surface wet-bulb potential temperatures (θ_w) over the city. However, θ_w is a reflection of both temperature and moisture inputs and only one of the case studies showed a relatively greater urban θ_w value attributable to a relative increase in urban moisture content. Moreover, of the foregoing investigators only Bornstein et al. (1972) have considered the vertical distribution of moisture through an urban-rural vicinity. They found that the urban area of New York City showed about a 4% relative increase in absolute humidity from the surface to 700 mb.

2.5 Urban Influence on Airflow

The effect of the airflow on convective cloud activity over an urban vicinity is a matter for wide speculation, and is usually contingent with the presence of the urban heat island. It is generally felt, and quite intuitively evident, that strong ambient winds will tend to rapidly ventilate the urban area. This has been documented by climatological studies in the literature (Sundborg, 1950; Duckworth and Sandberg, 1954; Landsberg, 1956; Kratzer, 1956; Mitchell, 1961; Chandler, 1965; Bornstein, 1968; Oke and Hannell, 1968; Clarke, 1969; and Munn et al., 1969). In addition, several of these authors have empirically determined critical wind speeds for particular cities at which the heat island vanishes (e.g., see Oke and Hannell, 1968). However, at moderately low wind velocities some investigators have noticed an "urban wind plume," which is in effect, a displacement of the urban heat island in a plume shape downwind of the city (Clarke, 1969; Munn et al., 1969). Similar to the urban heat plume concept, Summers (1965) developed a model which predicts a deeper adiabatic mixing layer over the city when compared to its rural surroundings. For cases of light winds, it has been suggested that the urban area may be capable of creating a solenoidal circulation with low-level convergence into the city's center and outflow aloft at its perifery (Okita, 1960; Pooler, 1963; Schmidt, 1963; Arnold, 1964; Hass et al., 1967; Angell et al., 1968; Georgii, 1968). To date conclusive evidence of an urban-induced solenoidal circulation is still lacking. Spangler (1972) reported that Project METROMEX 1971 data were inconclusive in discerning an urban-induced circulation.

2.6 Urban Influences on Turbulence

The increased roughness of the topography over a city will serve to increase the degree of mechanical turbulence. However, mechanical turbulence is small scale and is largely dissipated by viscous forces near the earth's surface (Taylor, 1952), a considerable distance below most convective cloud bases. Anderson (1971) concluded that frictional effects do not affect the depth of the mixing layer over an urban area, but that thermal turbulence is a contingent factor. Clarke (1969) showed, in his study of light wind cases, that thermal turbulence played a dominant role over mechanical turbulence. This has been corroborated in a theoretical study by Ball (1960). Atkinson (1970) concluded that mechanical turbulence was an insignificant factor in the triggering of a thunderstorm over London, and that the major contributors were thermal in nature. The effect of thermal turbulence on convective cloud activity has yet to be adequately investigated.

III. EXPERIMENTAL DATA AND PROCEDURES

3.1 General Description of St. Louis in Relation to Project METROMEX

The St. Louis area (Figure 3.1) was selected as the research site for Project METROMEX due to its smooth topography, distant separation from any large bodies of water, the availability of relatively good pre-existing climatological records, and the

fact that it is a fairly large city with a good deal of heavy industry. Meteopolitan St. Louis has a population of 1.5 million people with an additional 150,000 people in the East St. Louis, Illinois area and a combined population of 150,000 people in the Belleville-Collinsville-Edwardville-Alton, Illinois area.

The densely populated residential area (referred to in this paper as the "metropolitan area") and the principal downtown area with numerous buildings taller than 10 stories are shown on Figure 3.1. Heavy industry is located along both banks of the Mississippi River south of the confluence of the Mississippi and Missouri Rivers. The metropolitan area excluding the downtown area is laced with numerous deciduous trees. The vicinities surrounding the metropolitan area are primarily composed of woodlots and rolling farmland.

3.2 Explanation of Data Presentation

All times subsequently cited in this paper refer to Central Daylight Time (CDT). Radiosonde and aircraft spiral soundings are

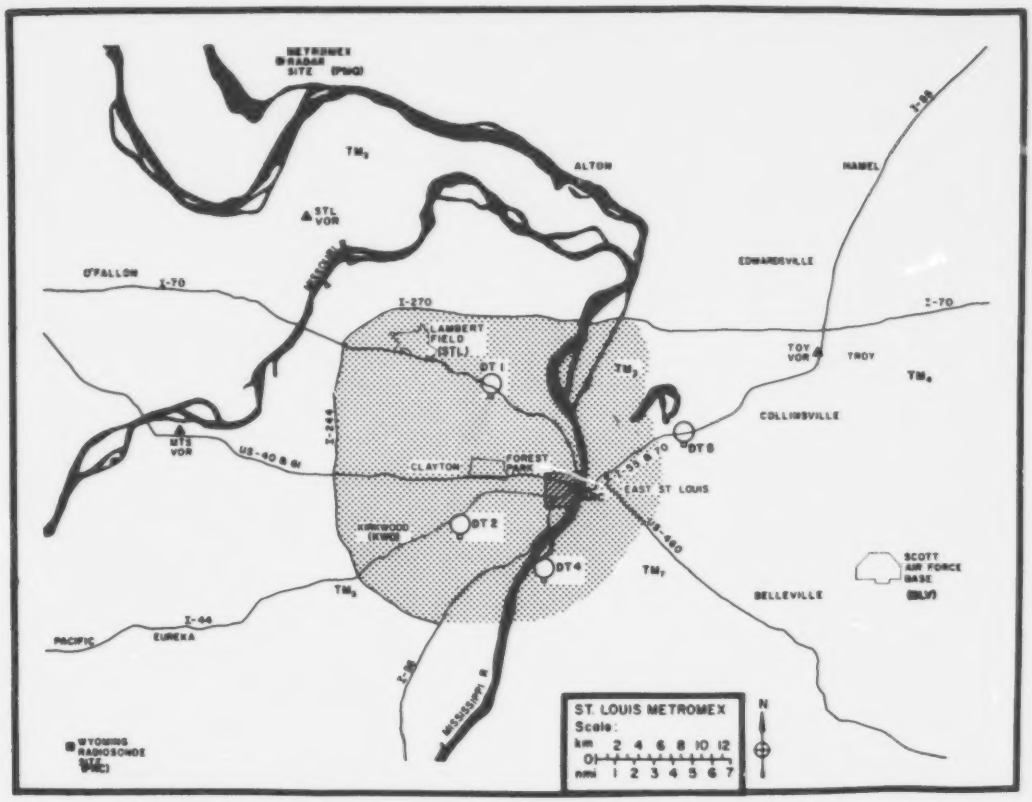

Figure 3.1. Pertinent geographical and operational sites within the greater St. Louis area. The more dense dot pattern corresponds to the downtown area and the less intense dot pattern shows the metropolitan area; a balloon symbol indicates a double theodolite site; the Illinois State Water Survey surface recording sites are shown by the symbol PM; and the three-letter identifiers indicate locations mentioned in the text. Double theodolite site #3 was located at the Jefferson National Monument, commonly called the Gateway Arch (ARC).

shown on a pseudo-adiabatic diagram with the right ordinate corrected to read pressure altitude. All heights cited in feet MSL are also corrected to pressure altitude. Where area-energy calculations were performed, the soundings were transcribed onto a tephigram so as to eliminate the inherent error of the non-conservative pseudo-adiabatic diagram. Since the aircraft spiral soundings were not executed to the surface, the low-level portion (typically 1000 ft AGL) of these soundings were extrapolated to known surface data. If surface potential temperature is greater than the interpolated potential temperature, a super-adiabatic temperature lapse is assumed in the lowest 200 ft above the surface (a typical value from the afternoon soundings examined during the month of August 1971 at St. Louis). The dew point trace has also been extrapolated in a similar manner. This trace is extended down a line of constant mixing ratio from the lowest point of the aircraft sounding to 200 ft AGL, and then drawn linearly from this point to the known surface value. All extrapolated traces are shown as dotted lines on the pseudo-adiabatic diagrams.

3.3 Surface Data

The University of Wyoming operated two instrumented mobile units (Chevrolet Carryalls) capable of measuring and recording nine different meteorological parameters. A complete description of this instrumentation may be found in Appendix A. Of primary interest to this research was the continuous measurement of temperature and dew point data from air sampled through an air intake located ~3 m above the surface. Data were recorded on a twenty-four channel chart recorder. The two mobile units were simultaneously calibrated in St. Louis prior to field operation. Transects were conducted which coincided with the track of the University of Wyoming aircraft, but the mobile units were also deployed via two-way radio to measure surface data at discrete locations beneath convective cloud activity. In addition, personnel operating the mobile units were equipped with 35-mm cameras and voice recorders facilitating the documentation of convective cloud activity.

Additional surface data were kindly provided by the Illinois State Water Survey from a network of seven temperature and dew point recording sites (Changnon, 1971). Supplementing these data were hourly observations taken by the National Weather Service station (NWS) at Lambert Field (STL) and (USAF) Air Weather Service personnel at Scott Air Force Base (BLV). Hourly observations were also recorded by four Air Weather Service double theodolite teams and by the University of Wyoming radiosonde crew near Pacific (PAC). Locations of the above mentioned sited are shown on Figure 3.1.

3.4 Aircraft Data

In order to effectively assess the influence of the St. Louis area on the modification of convective cloud activity, a knowledge of the vertical profile of meteorological parameters is also mandatory. This was accomplished via airborne measurement of data recorded on magnetic tape on board the University of Wyoming's updated C-45F/A twin engine Beechcraft aircraft. In addition, a real time display of certain meteorological parameters was available to the meteorologist on board the aircraft. Supplementary data were documented by the meteorologist in the form of event markers automatically recorded on the magnetic tapes, 35-mm photographs, and voice recorded notes. The magnetic tapes were computer processed yielding a continuous print out of all the recorded parameters and event markers. A description of the aircraft's instrumentation is given in Appendix B. The aircraft was also equipped with two-way radio providing continuous communication between the on board meteorologist, mobile unit crews and the Project METROMEX personnel located at the Pere Marquette (PMQ) radar site.

The aircraft flew multi-level transects with spiral soundings generally taken at the extremities of the transects. Additional spiral soundings were conducted in the vicinity of convective cloud activity when deemed appropriate by the on board meteorologist.

The aircraft system has been determined accurate to within $\pm$1.0C for temperature measurements, and $\pm$0.5C for dew point measurements (Appendix B). Radiosonde measurements of temperature and relative humidity (unsaturated ascent) are felt to be accurate to $\pm$1.0C and $\pm$5%, respectively (U. S. Air Force, 1955). However, Lenhard (1970) has found that the radiosonde delivers temperature information accurate to 0.3C, while Morrissey and Brousaides (1970) have found errors in humidity data of up to 15% when the sondes were exposed to a high degree of solar insolation.

Temperature and dew point data from a simultaneous aircraft spiral sounding and radiosonde launch over PAC on the morning of 9 August 1971 were compared in order to determine the compatibility of the two observing systems. Examination of the comparative traces showed that discrepancies were well within the cumulative total of the minimum errors documented in the literature (temperature $\pm$0.3C; relative humidity $\pm$5%).

3.5 Radiosonde and Wind Data

On operational days during the month of August, 1971, radiosondes were regularly launched from the University of Wyoming's PAC radiosonde site (Figure 3.1) at 0700 and 1230, and tracked to an altitude of 400 mb. The National Weather Service routinely tracked radiosondes to 700 mb at 0700 and 1230 from a downtown site at the Jefferson National Monument (Gateway Arch - ARC).

Double theodolite wind data were recorded by four Air Force Weather Squadron teams at locations shown in Figure 3.1. Additional wind data were accrued through:

1. single theodolite pibals conducted at 0000 and 1200 by the National Weather Service at Lambert Field,
2. 0700 and 1230 single theodolite pibals at PAC by University of Wyoming personnel,
3. single theodolite tracking of the 0700 and 1230 ARC radiosonde, and
4. single theodolite pibals recorded by mobile unit crews at selected locations.

Computer processing of the wind data was accomplished on the University of Wyoming's Sigma 7 and the computer facilities at the National Center for Atmospheric Research (NCAR) in Boulder, Colorado. Various smoothers were applied to the double theodolite data in order to reduce instrumentation and observer error (Spangler, 1972).

3.6 Radar Data

Mention of precipitation radar echo locations and tops in subsequent chapters of this paper were referenced from the transcribed field recordings of the University of Wyoming personnel attending the Illinois State Water Survey FPS-18 (10-cm band PPI) and TPS-10 (3-cm band RHI) radar systems. Additional radar data were available from microfilm records of the 10-cm band WSR-57 radar system operated at Lambert Field (STL) by National Weather Service personnel.

3.7 Lidar Data

Data of considerable value to the substance of this paper were produced by the Stanford Research Institute (SRI) Mark VIII lidar system, operated in conjunction with Project METROMEX. Descriptive details may be found in Uthe and Kealoha (1972).

IV. DESCRIPTIVE ANALYSES OF RESEARCH RESULTS

4.1 Research Approach

In the examination of convective cloud activity over the St. Louis area during the University of Wyoming's 1971 operational involvement in Project METROMEX, three days (23, 13, 9 August 1971) were selected as case study days on the merit of available comprehensive data. This section describes in detail synoptic conditions, spatial and time distributions of convective cloud activity, and comparative radiosonde soundings showing their relationship to convective activity for only the 23 August case study day; however, pertinent features from 13 and 9 August will be highlighted when relevant.

4.2 23 August 1971 Case Study

Synoptic Conditions. The St. Louis metropolitan area was under the influence of a high pressure air mass regime. There were no fronts within 150 n mi of the city at 0700 (Figure 4.1), and by 1900 the St. Louis area was still 50 n mi southwest of an old stationary front. At 0700, PAC and STL observers reported ground fog, smoke and haze, while the ARC observer did not report the presence of ground fog. By 0730, both PAC and STL were free of ground fog. Average winds recorded at PAC and the Air Force Pibal sites between 0600-0900 were 250° at 6 kts from the surface to 4500 ft MSL, and 030° at 12 kts from 4500-10000 ft MSL.

Cloud Coverage. The first appearance of convective cloud activity occurred at 1145 approximately 5 mi northeast of ARC as observed by personnel on board the University of Wyoming aircraft and mobile units. By 1200, a scattered regime of small cumulus clouds was present as shown schematically in Figure 4.2. A representative photograph of these clouds was taken at 1200 at ARC looking eastward (Figure 4.3). The eastern, western and northern boundaries of these clouds were confirmed by aircraft and mobile unit observations. These boundaries plus the observed wind patterns suggest that the clouds were not advected into the St. Louis area. From 1200-1400, this regime moved westward while tending to exclude the St. Louis metropolitan area as documented by the aircraft and mobile units. Cloud cover and tops increased gradually during this period as shown schematically in Figures 4.4 and 4.5. During the period from 1445-1630 the aircraft was not airborne; however, radar data from PMO showed no echoes and observers in the mobile units recorded no significant change in convective cloud activity. From 1645-1830, areas of isolated cumulonimbus cells appeared among the scattered to broken regime. Four cells were identified by radar

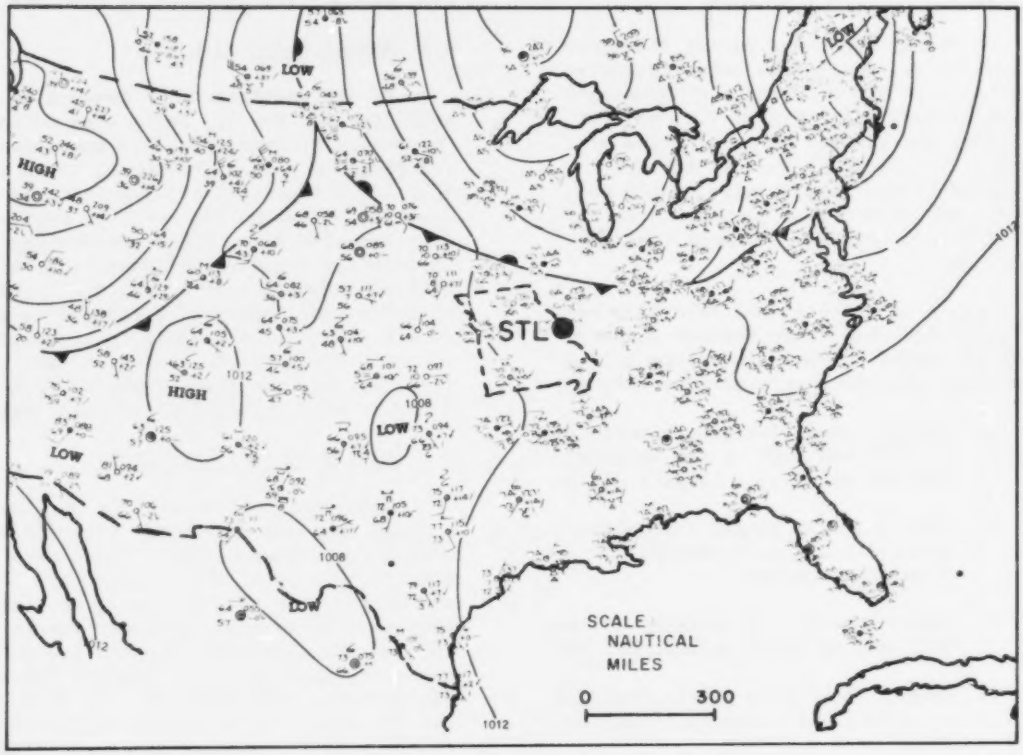

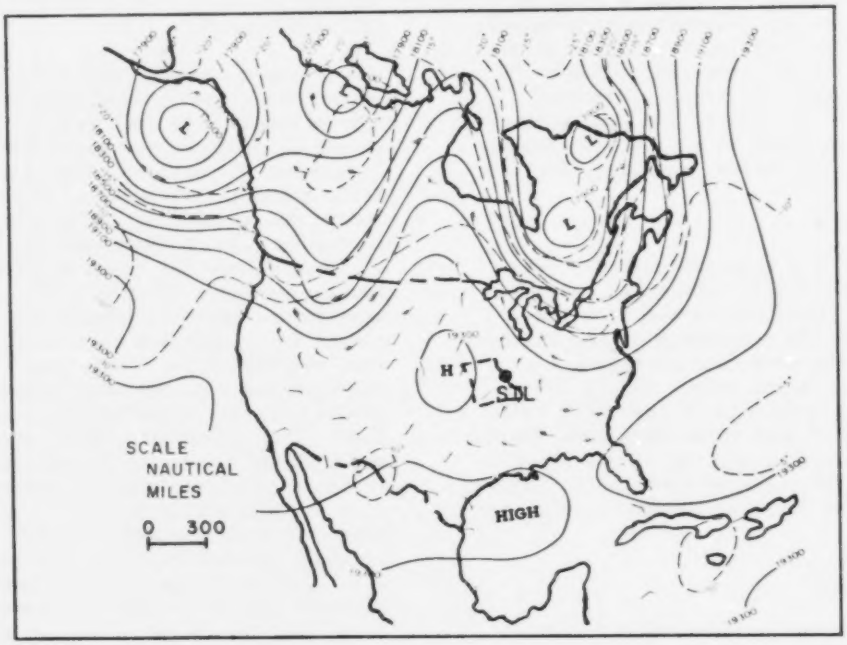

Figure 4.1. National Weather Service surface (top) and 500 mb (bottom) synoptic analyses for 0700 on 23 August 1971.

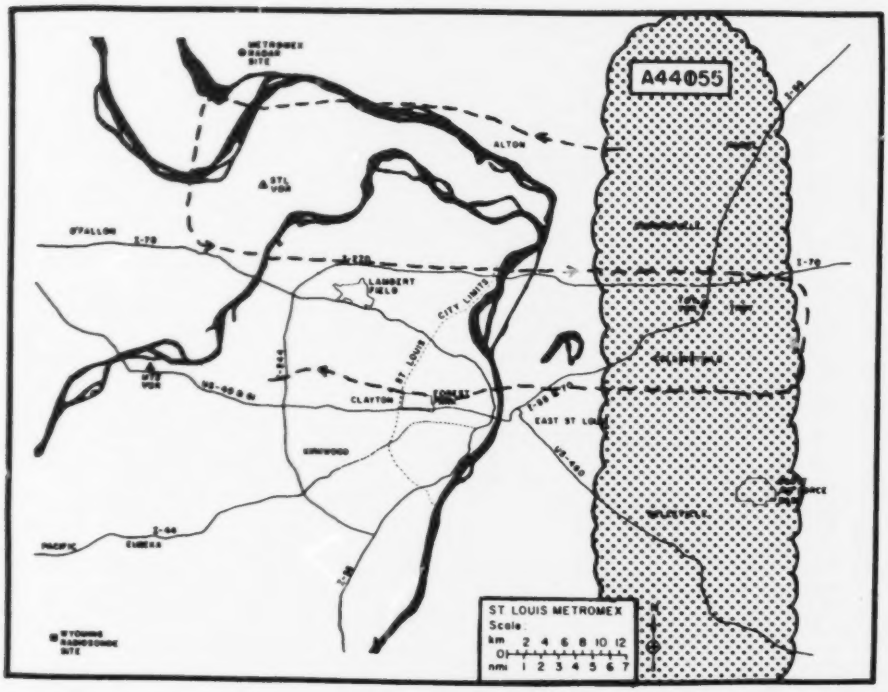
A44055
ALTON
O'FALLON
I-70
LAMBERT FIELD
CITY LIMITS
ST. LOUIS
CLAYTON
EAST ST. LOUIS
GRANITE CITY
I-64
I-55
I-270
I-255
I-44
I-55
I-70
I-64
I-55
I-270
I-255
I-44
I-55
I-70
I-64
I-55
I-270
I-255
I-44
I-55
I-70

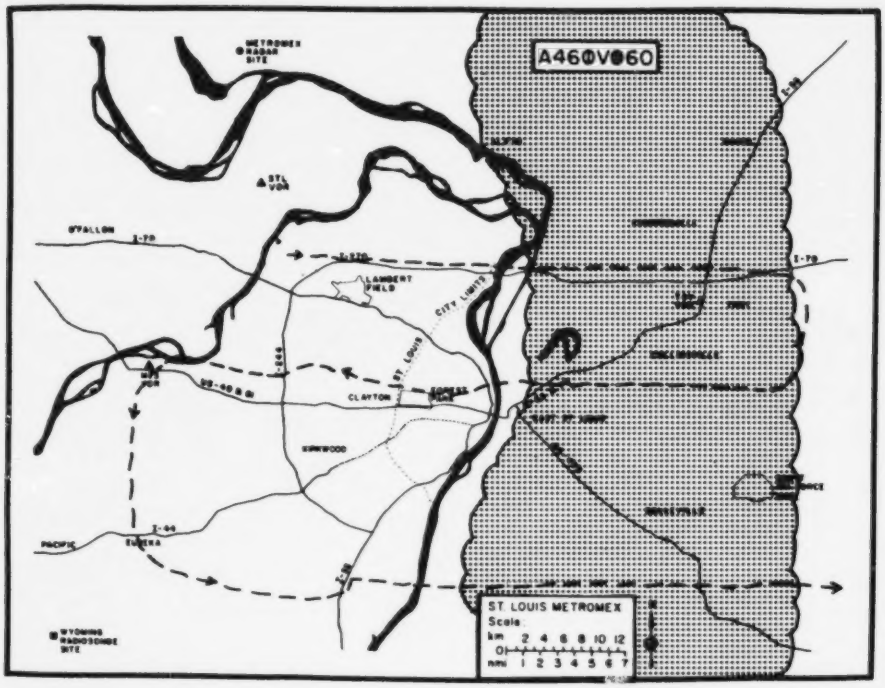

Figure 4.4. Schematic representation of cloud coverage at 1230 on 23 August 1971 with the aircraft flight track from 1200-1300 indicated by the dashed line and symbols explained in Figure 4.2.

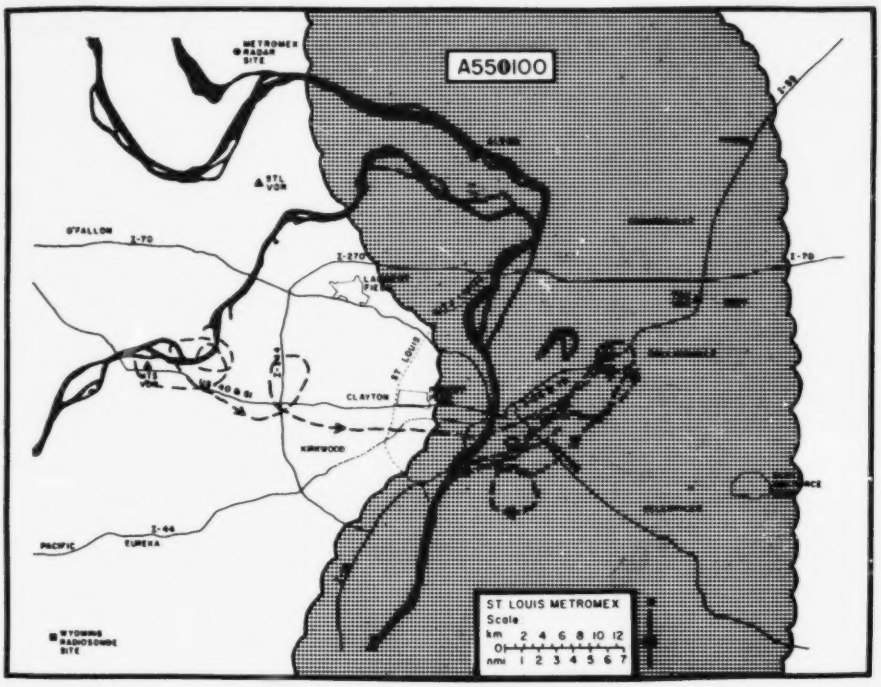

Figure 4.5. Schematic representation of cloud coverage at 1400 on 23 August 1971 with the aircraft flight track from 1330-1430 indicated by the dashed line and symbols explained in Figure 4.2.

aircraft and surface units and their locations are shown schematically on Figure 4.6. The PMQ radar reported the tops of these cells up to 36,000 ft and aircraft and surface observers recorded very light percipitation.

The salient descriptive features of 23 August 1971 are that

1. Convective cloud activity initiated east of the metropolitan area,

2. Convective cloud coverage moved slowly westward while tending to exclude the metropolitan area,

3. Three of the four cumulonimbus cells reported later in the day were located east through northeast of the metropolitan area, while the fourth was on the city's southern border,

4. The synoptic conditions fall into the category which Beebe and Morgan (1962) and Huff and Changnon (1972) have classified as the primary contributor to the summer precipitation anomaly.

Analysis of Convective Cloud Activity. At 1230 both PAC and ARC reported clear skies while small cumulus clouds were still forming to the immediate east of the Mississippi River (Figure 4.4). Inspection of the 1230 ARC radiosonde observation (Figure 4.7) between the surface and 870 mb (4400 ft MSL) shows a dry adiabatic temperature lapse rate, and a thermal profile above 870 mb which is conditionally unstable (lapse rate between dry adiabatic and saturated pseudo-adiabatic; stable to dry free convection). Therefore, a thermally buoyant air parcel rising from the surface must reach its convective condensation level (become saturated) below 870 mb in order for a convective cloud to form. Inspection of the dew point trace in Figure 4.7 confirms that there is insufficient moisture anywhere in the layer from the surface to 870 mb to facilitate condensation and supports the lack of observed convective activity.

The 1230 PAC radiosonde observations (Figure 4.8) shows a nearly dry adiabatic temperature lapse rate from the surface to 900 mb and a thermal profile from 900-860 mb which is absolutely stable to both dry and

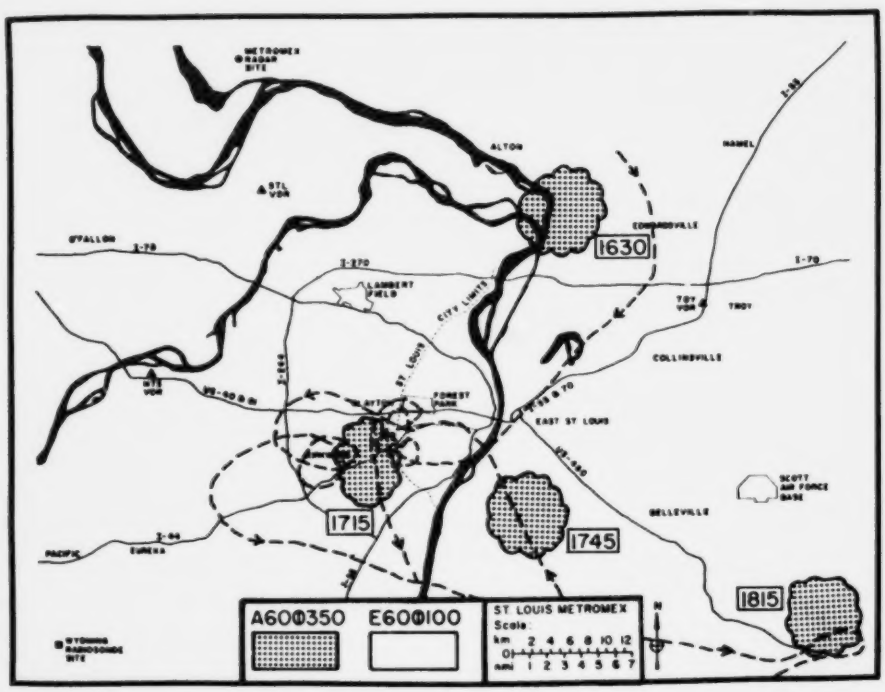

Figure 4.6. Schematic representation of cloud coverage with the time of observation of individual cumulonimbus, as noted by aircraft personnel, from 1630-1830 on 23 August 1971. PMQ radar indicated movement of the cells was generally from the northeast at 15 kts. The aircraft flight track from 1630-1830 is indicated by the dashed line and the symbols are explained in Figure 4.2.

saturated free convection (temperature lapse rate less than saturated pseudo-adiabatic). Therefore, parcel theory claims that convective cloud formation is impossible with the 1230 PAC temperature and moisture profiles, and supports the absence of any observed convective clouds.

It is evident from the foregoing analysis of the 1230 ARC sounding that two inhibiting factors must be modified before convective clouds are allowed to form over the area.

1. The dry adiabatic temperature profile (mixing or convection layer) must extend from the surface to a vertical height sufficient to provide condensation from the available moisture in the rising air parcel, or

2. Additional moisture must be supplied to an air parcel at some time during its ascent such that it will condense at or below the top of the existing mixing layer.

Of course, a combination of these two factors could serve to achieve the same effect. In the case of the 1230 PAC sounding, an additional obstacle must be overcome. Sufficient heating must be applied to the air column below 860 mb to eradicate the existing thermally stable layer from 900-860 mb.

Since small convective clouds were forming immediately east of the Mississippi River at 1230, analysis of an aircraft spiral sounding in clear air in the vicinity of these clouds taken at 1300 over Belleville, Illinois (BLV) from 953-860 mb will prove fruitful. Figure 4.9 shows this sounding with temperature and moisture traces extrapolated via the method described in Section III from 953 mb to surface data points recorded by a University of Wyoming mobile unit. Upon analysis it will become evident that all of the previously mentioned inhibition factors are absent in this sounding. The meteorologist on board the aircraft noted a visual cloud base of 4600 ft MSL (858 mb) and a corresponding cloud base temperature of 19C. A saturated mixing ratio of 16 g kg^{-1} is required for cloud formation at 4600 ft MSL. When this value is followed to the surface, it is seen to represent an average of the extrapolated moisture trace of only the lowest 200 ft AGL, and helps to explain the small vertical extent of cloud at that time.

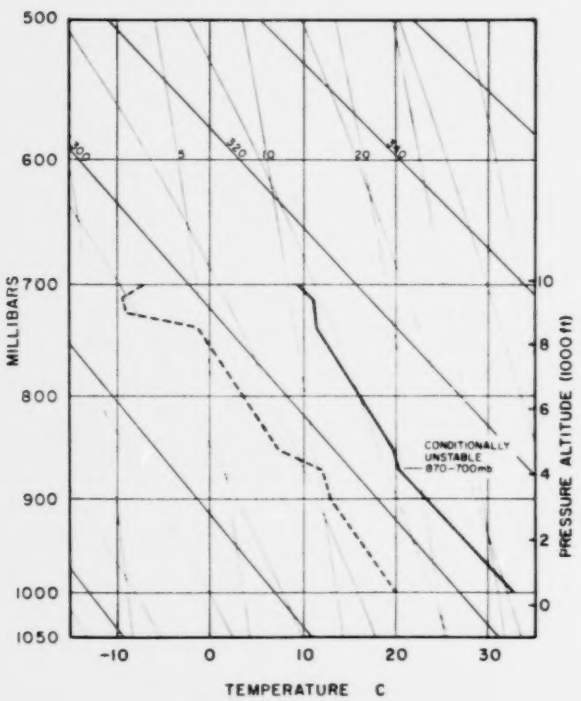

Figure 4.7. ARC radiosonde observation recorded at 1230 on 23 August 1971.

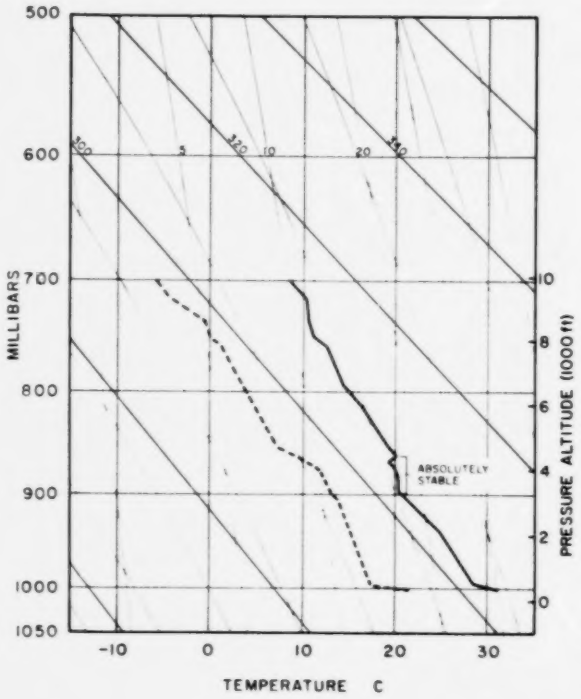

Figure 4.8. PAC radiosonde observation recorded at 1230 on 23 August 1971.

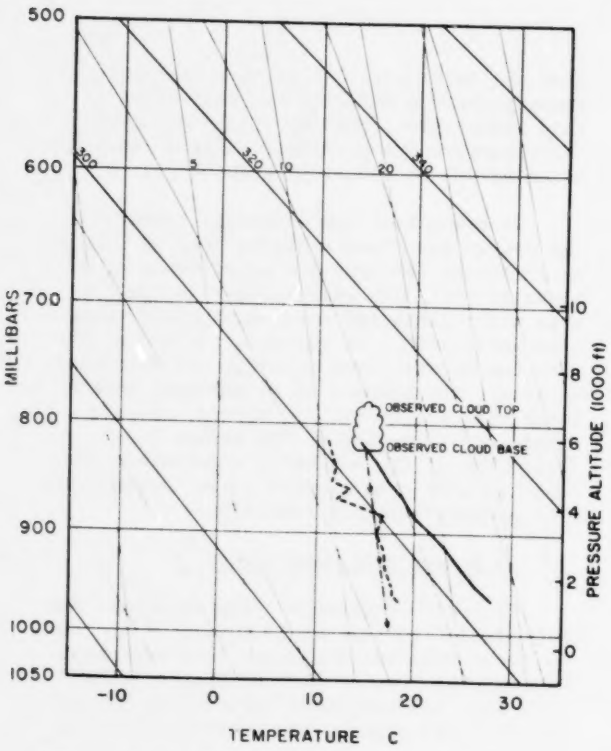

Figure 4.9. BLV aircraft sounding recorded at 1300 on 23 August 1971, showing the observed cloud bases and tops and the cloud base mixing ratio value extended to the surface.

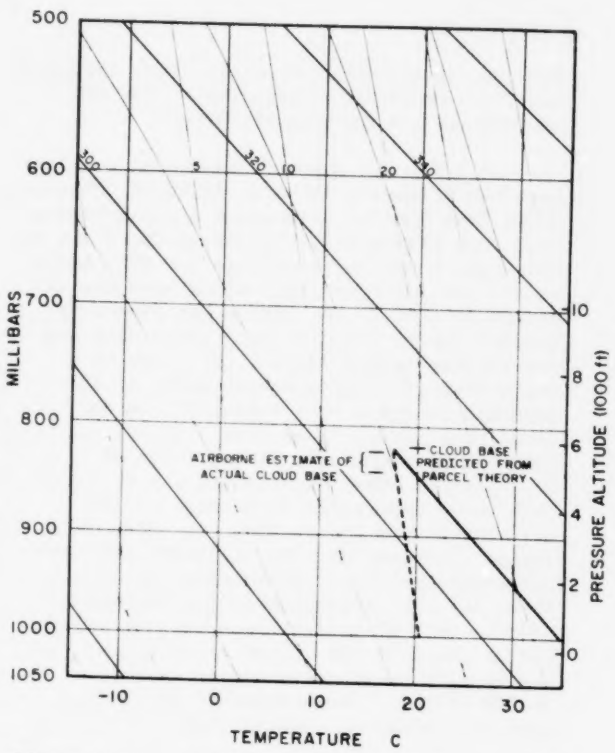

Figure 4.10. Cloud base predicted from parcel theory (using 1300 ARC surface temperature and dew point data) and the airborne observations of cloud base recorded over ARC at 1350.

Surface moisture is 1.5 g kg^{-1} greater at BLV than ARC and 2-4 g kg^{-1} greater in the 953-860 mb layer. Although the sounding over BLV was terminated at 860 mb, it can be seen that the top of the dry adiabatic temperature profile is at least 10 mb higher than PAC) and there is no inhibiting thermally stable layer below 860 mb. Thus, cloud formation via simple parcel theory with the 1300 BLV sounding was possible, but not with the 1230 ARC and PAC soundings.

Between 1300 and 1400 cloud cover had appeared over ARC. Although no soundings were taken in this time period, surface data recorded at ARC by the Illinois State Water Survey shows a surface temperature of 34.5C at 1300 with 16.2 g kg^{-1} of moisture; at 1400, these values were 35.5C and 15.2 g kg^{-1}, respectively. Using an average of the values, a buoyant parcel of air rising from the surface would reach its convective condensation level (CCL) at 5800 ft MSL (818 mb). From 1342-1352, the aircraft penetrated a series of small cumulus clouds in the vicinity of ARC during its 7500 ft MSL southwest-northeast transect across the metropolitan area. During these penetrations the meteorologist noted the stench from various surface effluents, suggesting that this air had indeed originated at the surface. At 1352, the meteorologist estimated cloud base over ARC at 5200-5700 ft MSL. Figure 4.10 shows the predicted cloud base from parcel theory and the observed cloud base. From these surface data and airborne observations, it seems probable that the dry adiabatic temperature profile had risen vertically approximately 50 mb (1600 ft), while low-level moisture had increased slightly (approximately 1 g kg^{-1}) from the 1230 ARC sounding. Both of these alterations were necessary in order for the observed convective clouds to have formed. Meanwhile the skies over PAC remained virtually cloud free until 1400 suggesting that the thermally stable layer observed on the 1230 PAC sounding (but not on the 1230 ARC sounding) was still inhibiting convective cloud formation.

The aircraft was not airborne from 1400-1620; however, the mobile unit crews were deployed to the eastern and western boundaries of the metropolitan area in order to take photographs and record observations. Convective clouds appeared to cover the entire metropolitan area while the sky was partially obscured due to haze and smoke. The greatest

vertical development of cumuli (some approaching the cumulonimbus stage) were over and to the east of the Mississippi River.

At 1650, the aircraft conducted a spiral sounding (Figure 4.11) over Kirkwood, Missouri (KWD) from 956-814 mb beneath a cumulonimbus cell (see Figure 4.6). Although there are no comparative earlier soundings for KWD, a few points are worth noting. Cloud base was reported at 6350 ft MSL with a corresponding temperature of 15.5C. Using these data and the surface data (Figure 4.11) taken by a University of Wyoming mobile unit, it is possible to again work downward from the cloud base data. Cloud base altitude and temperature dictates a mixing ratio of 12.8 g kg^{-1}. When extended to the surface, this value represents an average of the moisture in the lowest 2500 ft. With this deeper (compared with the 1230 ARC and 1300 BLV soundings) layer of moisture to draw from, and the strong supporting thermal profile with 3C positive buoyancy at 700 mb (using the 1230 ARC 700 mb temperature), one may justify the reported radar tops of 36,000 ft MSL. The adiabatic temperature profile and nearly constant mixing ratio from the surface to 815 mb show that both temperature and moisture are well-mixed in this layer; also, the top of the dry adiabatic temperature profile must have reached at least 805 mb (observed cloud base).

It seems that the principal feature of the convective cloud patterns over St. Louis on 23 August 1971 was the persistence of an elevated thermally stable layer in the PAC area which inhibited convective cloud formation until 1400. At the opposite end of the city convective cloud activity had initiated by noon. The absence of an elevated stable layer east of the city by midday, and the subsequent deepening of the mixing layer (extension of the adiabatic temperature profile) in that area appears to be commensurate with convective cloud formation.

4.3 13 August 1971 Case Study

Synoptic Conditions. The situation was very similar to that of 23 August 1971. The St. Louis area was subjected to a high pressure air mass regime with no fronts within 400 n mi. Average winds recorded at PAC and the Air Force pibal sites between 0600-0900

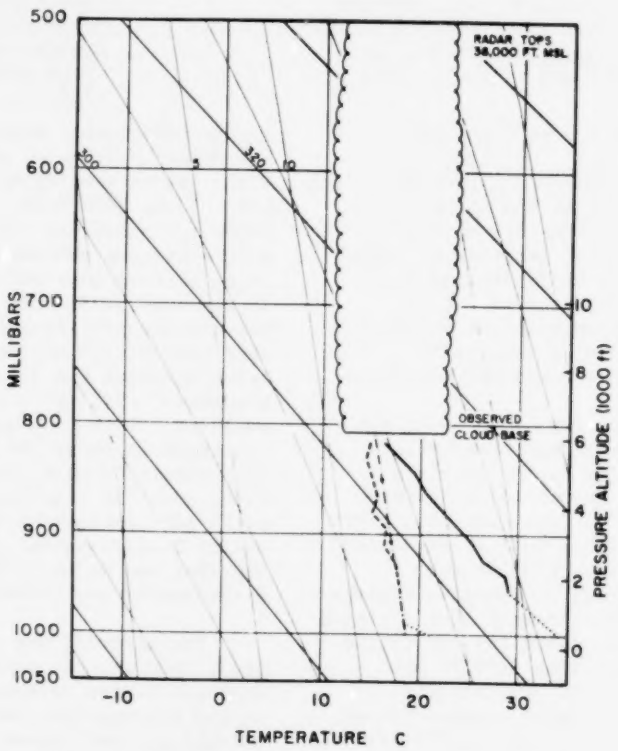

Figure 4.11. KWD aircraft sounding recorded at 1650 on 23 August 1971, showing a schematic representation of observed clouds with cloud base mixing ratio value extended to the surface.

were 250° at 5 kts from the surface to 4500 ft MSL, and 020° at 10 kts from 4500-10000 ft MSL.

Cloud Coverage. The significant descriptive features of the cloud coverage on 13 August 1971 are summarized in the following:

1. An early morning altostratus layer was less dense over the PAC area and was erradicated at least one hour before (0930) the layer over and to the east of the city,

2. Small cumulus clouds (vertical depth ∿1500 ft) appeared over the entire St. Louis area at approximately the same time (∿1300),

3. This convective activity dissipated rapidly over and to the east of the St. Louis metropolitan area (with the metropolitan area showing less dense sky coverage at all times), while cumulus clouds west of the city grew to substantial heights (25,000 ft) and

4. The synoptic conditions fall into that category which Beebe and Morgan (1972) and Huff and Changnon (1972) have classified as the primary contributor to the summer precipitation anomaly.

Analysis of Convective Cloud Activity. As for the case study of 23 August 1971, the existence of an elevated stable layer on 13 August 1971 played a predominant role in the location of convective cloud activity. However, in this case the stable layer did not initially inhibit the formation of convective clouds but instead, it selectively snuffed their development, and then eventually their formation. Of additional interest is the fact that the locations of inhibition and development of convective cloud activity on 13 August 1971 were the reverse of the 23 August 1971 case study.

4.4 9 August 1971 Case Study

Synoptic Conditions. Again the St. Louis area was under the influence of a high pressure air mass regime, with no major fronts within 800 n mi. However, the temperature and dew point temperature of Springfield, Missouri, located southwest (upwind) of St. Louis were respectively 5F and 11F lower than the St. Louis value. Therefore, the possibility of an existing cold dry line located approximately 200 n mi southwest of St. Louis should not be excluded. Average winds recorded at PAC and the Air Force pibal sites between 0600-0900 were 250° at 8 kts from the surface to 10,000 ft MSL.

Cloud Coverage. The noteworthy descriptive features of cloud coverage on 9 August 1971 are as follows:

1. Convective cloud activity was primarily limited to an area immediately east of the St. Louis Metropolitan area,

2. Cumulonimbus cells (Figure 4.12) formed in the area immediately east of the metropolitan area while a virtually clear regime existed over and to the west of the metropolitan area and

3. The synoptic conditions fall into that category which Beebe and Morgan (1972) and Huff and Changnon (1972) have classified as the primary contributor to the summer precipitation anomaly.

Analyses of Convective Cloud Activity. The descriptive analysis of the 9 August 1971 data has again pointed to the vertical temperature structure as the key feature in the spatial distribution of convective cloud activity. Although there was no sharply defined elevated stable layer at midday on 9 August 1971 the ascendent of potential temperature from the surface to 850 mb in the PAC area, and the strictly adiabatic temperature lapse rate in the corresponding layer at the opposite end of the city were commensurate with the location of convective cloud activity.

4.5 Composite Analysis of Convective Cloud Activity

The foregoing descriptive discussions provide an area for comparative analysis. The salient features of convective cloud activity on the three case study days are summarized in the following:

1. The synoptic conditions on all three days are representative of the climatological assessment of the summer precipitation anomaly documented by Beebe and Morgan (1972) and Huff and Changnon (1972).

2. There existed preferential areas of convective cloud activity in the St. Louis vicinity on all three case study days.

3. Recorded oder from surface effluents suggests that the inflow air at cloud base possessed a surface origin.

Figure 4.12. Small cumulonimbus in the vicinity of the TOY VORTAC at 1225 as seen from Forest Park.

4. Convective cloud activity was associated with a dry adiabatic temperature lapse rate (mixing or convection layer) from the surface to cloud base, and sufficient low-level moisture to establish a CCL at the top of this air column.

5. The preferential areas of convective cloud activity coincided with the temperature and moisture profile requirements cited above in #4.

6. Absence of convective cloud activity (while other areas of close proximity in the urban vicinity produced clouds) was characterized by a lack of the thermal or moisture profile cited in #4.

7. These areas of inhibited convective cloud activity were always associated with a thermally stable layer in the vicinity of the CCL (determined by observations from convective activity in the preferential region), and in two of the three cases (23 and 13 August 1971), this layer was stable to both dry and saturated convection (absolutely stable).

It seems evident that a characteristic feature of those soundings which did not support convective cloud activity is the presence of an elevated thermally stable layer. On the afternoon soundings, this layer is shown capping a layer of dry adiabatic temperature lapse rate (mixing layer). Stable layers of this type have also been documented by other investigators (Davidson, 1967; Olsson et al. 1971; Spangler, 1972).

In order to determine that the stable layers observed on these case study days were

not a rarity, all days when comparable soundings were available for ARC and PAC during August 1971 were analyzed. Both the 0700 and 1230 soundings were examined for stable layers from 900 to 700 mb. The presence of a stable layer was determined from the following criteria:

1. Ascendent of potential temperature greater than 2K and

2. A temperature lapse rate less than saturated pseudo-adiabatic.

These criteria were established because the temperature of a buoyant air parcel (thermal) is characteristically less than 2K greater than environmental air (Malkus, 1955; Warner and Telford, 1967), and the fact that a saturated pseudo-adiabatic environmental temperature lapse rate is stable to both dry and saturated convection. This analysis showed that elevated stable layers were present 11 of 12 days on the 0700 ARC and PAC soundings, and 9 of 12 days on the 1230 ARC and PAC soundings (these data should not be construed to imply that stable layers were simultaneously present at both locations). Therefore, the presence of elevated stable layers was a dominant feature of the morning and noon soundings.

Returning to the three case study days, Table 4.1 was prepared to elucidate the correlation between adiabatic mixing layers, elevated stable layers, and the location of convective cloud activity. This table shows that the convective cloud activity was always in nearest proximity to the sounding characterized by an adiabatic mixing layer below the CCL, and the absence of an elevated stable layer. Inhibition of convective activity was always associated with the absence of an adiabatic mixing layer below the CCL, and in two of the three cases, the existence of an elevated stable layer. An investigation into the mechanisms involved in this anomaly seem appropriate.

V. MECHANISTIC ANALYSIS OF RESEARCH RESULTS

5.1 The Approach

Data from the preceding section suggests that an urban area may be related to elevated stable layers and associated convective cloud activity. This section will examine possible mechanisms connected with the formation and development of elevated stable layers for the three case study days.

5.2 23 August 1971 Case Study

Elevated Heating Profile. Inspection of the 0700 ARC and PAC soundings (Figures 5.1 and 5.2) reveals the existence of an elevated stable layer present at ARC at 860 mb, while PAC shows an elevated stable layer based at 870 mb. Morning soundings were also routinely taken by the National Weather Service at Salem, Illinois (SLO), 60 n mi east of St. Louis, and Monett, Missouri (UMN), 220 n mi southwest of St. Louis. Neither of these soundings showed the characteristic temperature inversion between 900-800 mb found on both the ARC and PAC soundings. A survey of the morning surface and 500 mb charts (Figure 4.1), and the morning 850 mb analysis (Figure 5.3) show

Table 4.1. Relationship between elevated stable layers, adiabatic mixing layers (from the surface to cloud base), and the location of primary convective activity for the three case study days.

		MORNING		MIDDAY		
Date (Aug)	Site	Elevated Stable Layer	Adiabatic Mixing Layer	Elevated Stable Layer	Adiabatic Mixing Layer	Location of Primary Convective Activity
23	PAC	yes	no	yes	no	East of ARC
	ARC	yes	no	no	yes	
13	PAC	yes	no	no (1530 PAC) yes (1600 TOY)	yes	PAC
	ARC	yes	no		no	
9	PAC	yes	no	no	no	East of ARC
	ARC	no	no	no	yes	

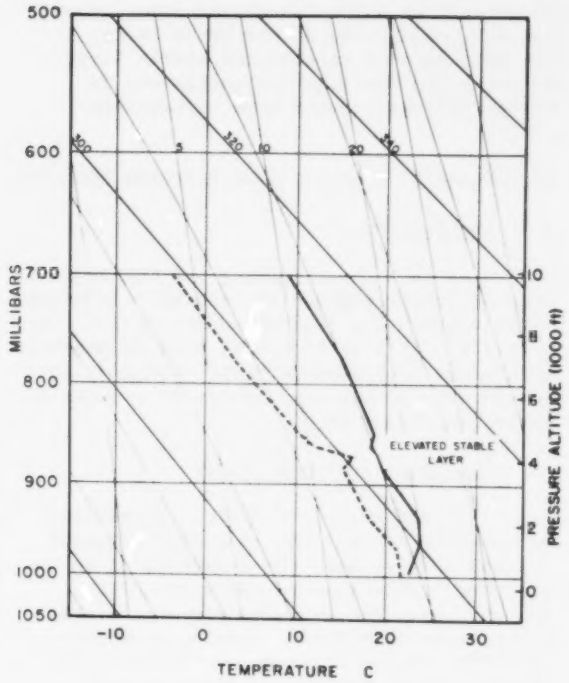

Figure 5.1. ARC radiosonde observation recorded at 0700 on 23 August 1971.

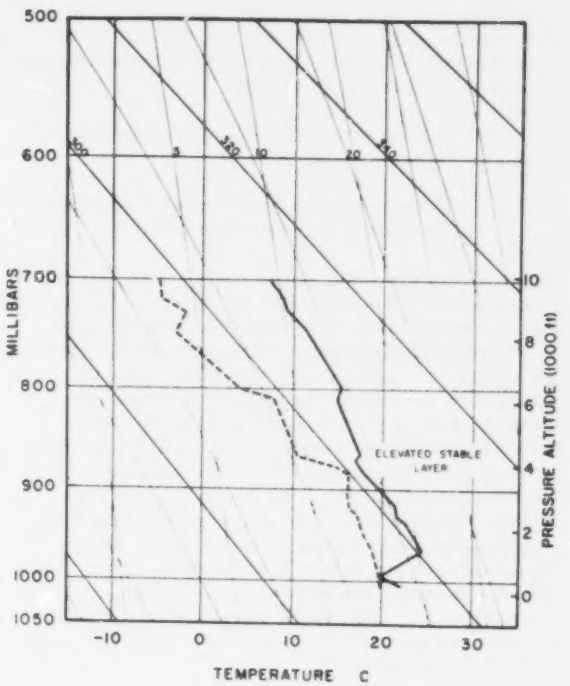

Figure 5.2. PAC radiosonde observation recorded at 0700 on 23 August 1971.

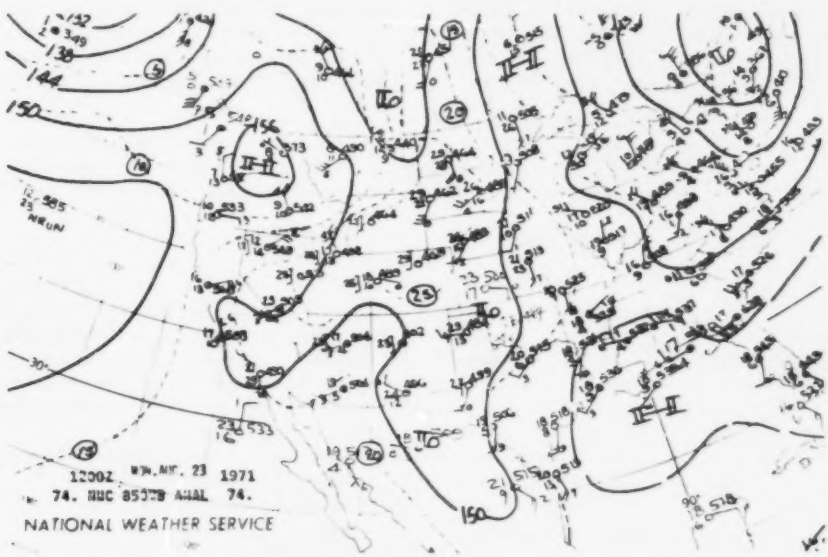

Figure 5.3. National Weather Service 850 mb synoptic analysis for 0700 on 23 August 1971.

no significant pressure or thermal gradients between these stations suggesting that all four locations were subjected to the same high pressure air mass regime. This is further substantiated by Table 5.1 which compares the mean potential wet bulb temperature ($\bar{\theta}_w$) in the respective 900-800 mb layers for the four stations, a familiar method for identifying a common air mass (Saucier, 1955). Since all four stations appear to be situated within a common air mass, and only ARC and PAC exhibited elevated stable layers between 900-800 mb, it would seem that the St. Louis urban area may have had a causal effect on the vertical temperature structure in that layer.

From 0700 to 1230, both ARC and PAC were subjected to heating from solar insolation. A planimeter analysis (area-energy evaluation on a tephigram) of the magnitude of heating in layers between 1000-800 mb over ARC and PAC was made in order to compare relative differences at the stations. Figure 5.4 shows the amount of warming in joules kg^{-1} from 0700-1230 over ARC and PAC in the layers: 1000-950, 950-900, 900-850 and 850-800 mb. These data are also shown in tabular form in Table 5.2.

The salient feature of this comparison is the fact that the ARC sounding warmed principally in the lower 100 mb, while PAC showed substantial elevated warming in the 900-800 mb layer. The differential heating through the vertical at PAC (i.e., elevated warming) has created somewhat of a "skewed hour glass" heating profile between the 0700 and 1230 soundings in the 1000-800 mb layer. The 1230 PAC temperature profile, with its associated elevated stable layer due to elevated warming, was the principal inhibiting factor to the formation of convective activity over PAC. Meanwhile, heating of the morning ARC sounding from 0700-1230 did not show this magnitude of elevated warming and thus supported convective cloud activity after 1230. An investigation into possible explanations of the formation of this discontinuity now seems appropriate.

Advection in the Vicinity of an Elevated Stable Layer. Data from the work of Baynton (1968), Olsson et al. (1971) and Spangler (1972) have shown that elevated stable layers which cap a mixing layer are associated with a wind shift (typically veering) and velocity minimum through the vicinity of the stable layer, followed by a wind velocity increase as the profile proceeds upward in the vertical. These findings are supported by the following data.

Table 5.1. Mean wet bulb potential temperatures ($\bar{\theta}_w$) in the respective 900-800 mb layers computed from 0700 23 August 1971 radiosonde data.

	ARC	PAC	SLO	UMN
900-800 mb layer $\bar{\theta}_w$ (K)	292.5	292.0	292.0	292.5

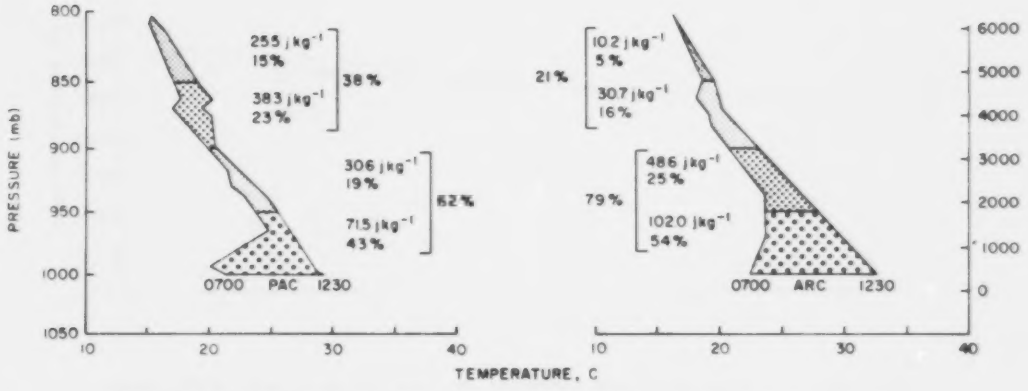

Figure 5.4. Heating profiles from 0700-1230 at PAC and ARC on 23 August 1971.

Table 5.2. The amount of warming in joules kg^{-1} of 50 mb layers from 1000-800 mb between 0700-1230 at PAC and ARC.

Layer	Magnitude of Heating ($j\ kg^{-1}$)		Percent by Layer			
	PAC	ARC	PAC		ARC	
850-800	25.5	10.2	15%	} 38%	5%	} 21%
900-850	38.5	30.7	23%		16%	
950-900	30.6	48.6	19%		26%	
1000-950	71.5	102.0	43%	} 62%	53%	} 79%
1000-800	165.9	191.5	100%		100%	

At 0730 simultaneous pibal launches were conducted by University of Wyoming personnel at PAC and Air Force teams at sites DT2 and DT4 (see Figure 3.1 for locations). Inspection of these wind data presented in Figure 5.5 shows that the winds from 960-890 mb were from the west to southwest and generally decreasing in velocity at all three locations. However, from 890-865 mb the wind profile over PAC exhibits a wind velocity minimum, shift in direction to northeast, and a subsequent wind velocity maximum. At DT4 these same events start to occur at 860 mb, or approximately 30 mb higher than the PAC profile, while the DT2 profile does not show any of these characteristics up to the termination of the track at 825 mb. A sloping elevated stable layer, as analyzed from the above wind data, is also shown on Figure 5.5. Figure 5.6, which displays the 0700 ARC and PAC soundings, shows the base of the actual elevated stable layer over ARC (860 mb) to be 10 mb higher than the base at PAC (870 mb). Thus, radiosonde data shows that the elevated stable layer probably slopes downward approximately 10 mb from ARC to PAC at 0700. The 0730 wind data supports this general picture, but suggests a greater degree of downward sloping (~30 mb) toward the PAC area. The possibility of some dynamical influence in the PAC area, which is lowering the effective base of the elevated stable layer (shrinking the potential depth of the mixing layer) is implied from these temperature and wind data.

The scheduled 0900 pibals were tracked to only 900 mb at sites DT2 and DT4, and to 700 mb at PAC. These wind data displayed the same wind profiles as the 0730

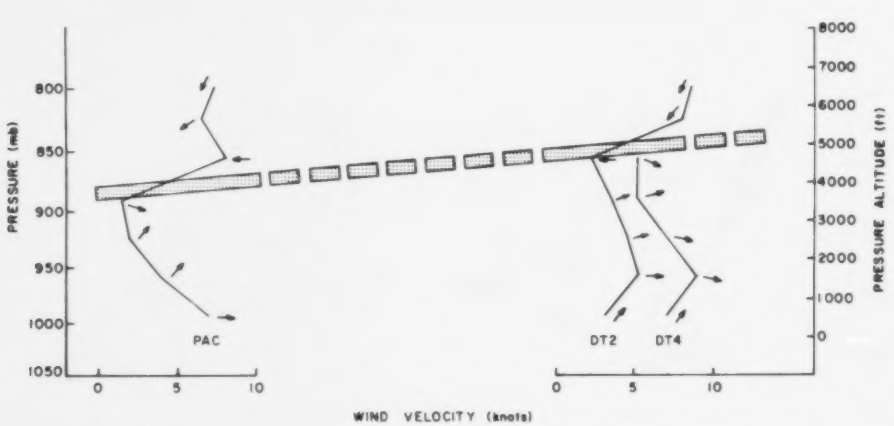

Figure 5.5. Wind profiles recorded at 0730 on 23 August 1971 with arrows indicating wind direction and sloping elevated stable layer.

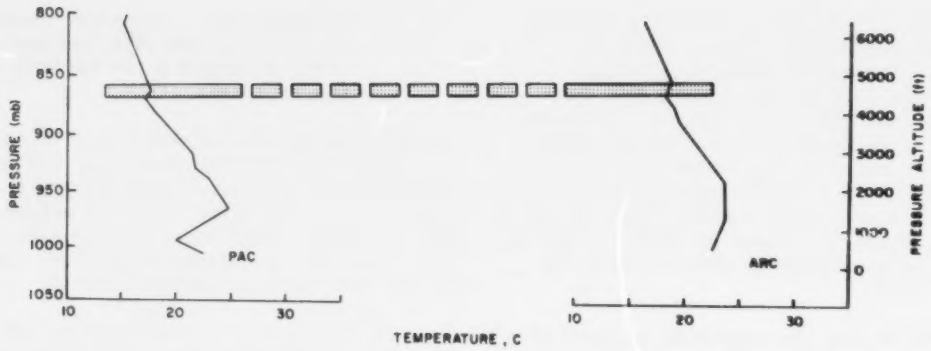

Figure 5.6. Thermal profiles recorded at PAC and ARC at 0700 on 23 August 1971 showing the sloping elevated stable layer.

releases (the wind data over PAC again indicated the height of the elevated stable layer between 890 and 870 mb), implying that the 0730 wind profiles were probably persistent to at least 0900. A further look at Figures 5.5 and 5.6 shows, in general, relatively warmer air is being advected above the top of the sloping elevated inversion from northeast to southwest (ARC to PAC) and relatively cooler air is being advected in the opposite direction at altitudes below the elevated stable layer (except for a very shallow layer from 965-950 mb). The mean transport wind below the base of the sloping elevated stable layer was calculated to be 260° at 6 kts, which results in about a 5-hour travel time from PAC to ARC. Since the sounding at PAC is probably characteristic of the air in some radius around that discrete location, this travel time represents a maximum value. However, ARC was subjected to a greater relative and absolute magnitude of heating that PAC in the 1000-900 mb layer from 0700 to 1230 (see Figure 5.4 and Table 5.2). Therefore, cool air advection from PAC to ARC in this level would tend to counter the observed heating trend. Above the base of the sloping elevated stable layer, the mean transport wind was calculated to be 060° at 7 kts, resulting in a maximum travel time of approximately 4 hours. By 1130, the wind profiles recorded at DT2, DT4 and ARC were all light (3 kts or less) and quite variable from the surface to 700 mb, indicating no systemized flow in the St. Louis area.

Due to the thermal ascendent of potential temperature upward through an elevated stable layer and the resultant density discontinuity, air that is being advected horizontally across the top of the stable layer will generally follow its upper contour. If air had been advected across the top of the elevated stable layer shown in Figure 5.6 from ARC to PAC, it should maintain its potential temperature provided there were no heat sources or sinks. The potential temperature at the top of the elevated stable layer (850 mb) on the 0700 ARC sounding shows a value of θ = 306.0K. The potential temperature at the top of the elevated stable layer (860 mb) on the 1230 PAC sounding is also θ = 306.0K. This suggests that a portion (860-800 mb) of the elevated warming in the 900-800 mb layer at PAC may have been due to warm air advection along the top of the elevated stable layer (Figure 5.7). However, this does not explain the warming in the 900-860 mb region below the elevated stable layer at PAC since the 1230 PAC sounding is everywhere warmer than the 0700 ARC sounding in that layer. One should also notice (Figure 5.7) that the 0700 and 1230 PAC soundings are nearly coincident above 800 mb, prohibiting the implication that the warming in the 900-800 mb layer was due to large scale synoptic subsidence.

Since the elevated warming of the PAC sounding from 0700-1230 in the 900-860 mb layer cannot be explained by simple horizontal advection, consider the possibility that air above the elevated stable layer penetrated downward through this stable layer in the vicinity of PAC. If this occurred, then the effect of adiabatic compressional heating could serve as a mechanism which would contribute to the observed warming below the elevated stable layer at PAC.

Recall from the above discussion that relatively warmer air was being continuously advected from the ARC vicinity, along the top of the sloping elevated stable layer, to the PAC area. If this potentially warmer air being advected across the top of the elevated stable layer penetrated downward through it, one would expect to see, at any given time, a gradient of potential temperature below the elevated stable layer which reflects the mixing of the "entrained" (warmer) air from above and the "recipient" (cooler) air below the elevated stable layer.

In order to elucidate upon this concept, consider the sequential process shown in Figure 5.8. The dashed temperature trace at the extreme left is the actual 0700 PAC sounding for the 900-800 mb region. Proceeding chronologically from this diagram toward the right, warmer air from above the elevated stable layer as it proceeds southwestward from ARC is being theoretically mixed into the recipient air below the elevated stable layer at PAC. This is accomplished theoretically in Figure 5.8 by:

1. Pro-rating the magnitude of warm air advection above the elevated stable layer from ARC with time,

2. Continuously mixing this warm air uniformly through the elevated stable layer, and

3. Bringing this "entrained" warm air downward at constant temperature until it matches the temperature of the recipient air.

The diagram at the extreme right in Figure 5.8 shows the 0700 PAC sounding, and the theoretically predicted temperature trace over PAC at 1230 along with the actual 1230 PAC sounding. Good agreement is seen between the predicted and actual 900-800 mb segments of the two temperature profiles.

In a further consideration of the ramification of this process, we will first define the potential depth of the mixing layer (from subsequent solar insolation at the surface), as the depth from the surface to the base of the elevated stable layer. If warm air did penetrate downward through the

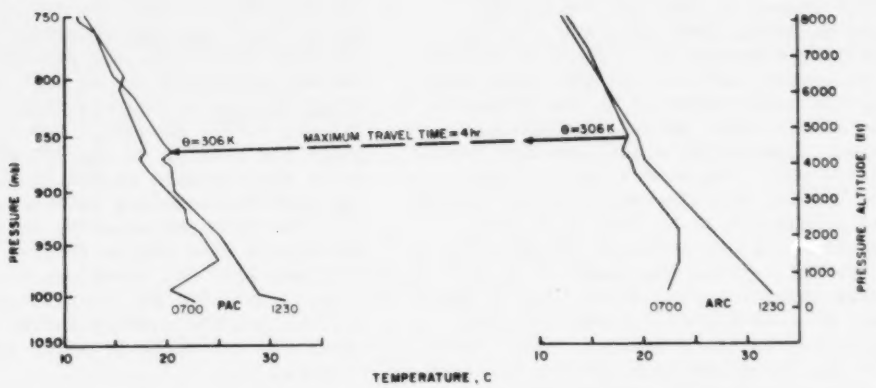

Figure 5.7. Heating profiles between 0700-1230 at PAC and ARC on 23 August 1971 indicating possible warm air advection above the sloping elevated stable layer.

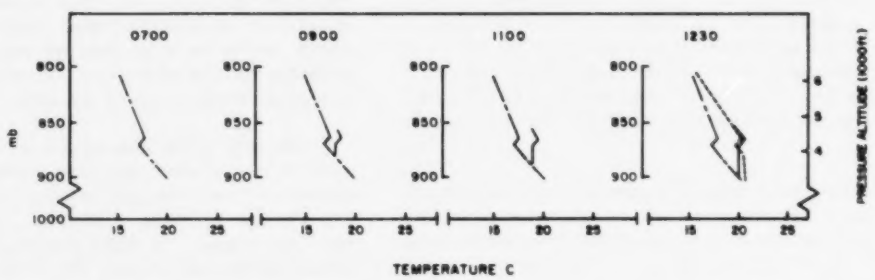

Figure 5.8. Hypothesized thermal profile (solid line) derived from pro-rating the entrainment of air downward through the elevated stable layer on the 0700 PAC radiosonde observation (broken line), with a comparison of the actual 1230 PAC radiosonde observation (dashed line).

elevated stable layer between 0700 and 1230 at PAC, it would result in the apparent shrinking of the potential depth of the mixing layer at PAC. This is indeed what was observed over PAC as the base of the elevated stable layer was located at 870 mb on the 0700 sounding, while on the 1230 sounding it is shown capping the mixing layer at 900 mb. There was no elevated stable layer present on the 1230 ARC sounding; however, the top of the (adiabatic) mixing layer was at 870 mb, or 10 mb below the base of the elevated stable layer found on the 0700 ARC sounding. As a consequence, the top of the mixing layer sloped downward from ARC to PAC at 1230 with a differential of 30 mb (Figure 5.9). An additional point of interest is the fact that this differential (30 mb) in the top of the mixing layer between ARC and PAC at 1230, is the same degree of slope (30 mb) found in the elevated stable layer as analyzed from 0730 wind data (Figure 5.5).

Returning to the implications of the proposed penetration (entrainment) of warm air through an elevated stable layer (and the resultant shrinking of the potential mixing layer depth), one should notice that the area of primary convective activity on 23 August 1971 coincided with the general location of the deepest mixing layer at 1230. On the other hand, the relatively shallower mixing layer at PAC, with its associated elevated stable layer, inhibited the formation of convective activity in that vicinity. Supporting evidence for this observation was found in a climatological analysis of the 1971 Project METROMEX data by Beebe and Morgan (1972), where it was shown that the area of relatively enhanced precipitation in the St. Louis area was associated with a deep mixing layer. They saw a sharp increase in rainfall when the midday mixing layer depth at ARC (as analyzed by the method of Weurch, 1971) was equal to or greater than 5000 ft. In his Project METROMEX case study of 18 August 1971, Spangler (1972) found (using continuous mobile lidar data) that the area of primary convective cloud activity corresponded with the location of the deepest mixing layer depth. In addition, he saw an elevated stable layer at 0700 on 12 August 1971 which was horizontal between ARC and PAC, but subsequently lowered 40 mb at PAC by 1230 while maintaining its initial (0700) height at ARC. This resulted in a differential of 40 mb in mixing layer depth between ARC and PAC, an occurrence quite similar to the case of 23 August 1971 (however, the persistence of the elevated stable layer at both locations served to inhibit convection over the entire St. Louis area on 12 August 1971).

An inhibition to convective cloud activity appears to be contingent upon the existence of an elevated stable layer, and the effect it may have on the potential mixing layer depth via an elevated heating process. Since our interpretation of the elevated heating process on 23 August 1971 could not be explained solely through the horizontal advection of warm air, and the foregoing analyses suggest a mechanism where the phenomenon may be elucidated by the penetration of warm air downward through an elevated stable layer, an examination concerning the feasibility of this process will be presented.

Vertical transport of Air Through an Elevated Stable Layer. It is often beneficial to model meteorological events using a fluidal similitude. A thermally stable layer, or temperature inversion, through the vertical in the atmosphere is comparable to a density gradient in an incompressible fluid. This gradient of density is also present in the atmospheric system if one were to compare air densities above and below the stable layer.

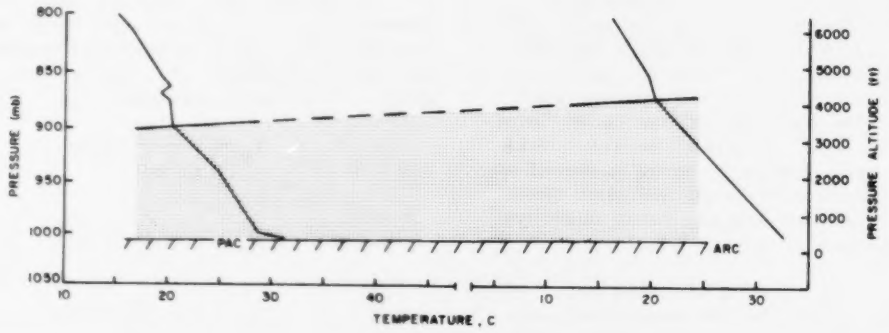

Figure 5.9. Thermal profiles at PAC and ARC at 1230 and the derived mixing layer.

Along these lines, Rouse and Dodu (1955) constructed an experimental model consisting of saline water underlying pure water. The two layers were separated by a density gradient. When turbulent kinetic energy was generated in the upper layer by means of an oscillating grid, an unexpected result occurred. Instead of penetrating far enough into the lower stratum to form a buffer zone as anticipated, the turbulence did not penetrate at all, but produced "interfacial cusps from which streamers were rapidly lifted and diffused through the upper stratum." As this "entrainment" process continued, the interface lowered as the concentration of the upper layer increased, while the layer below the interface remained undisturbed.

Ball (1960) investigated the possibility of applying the experimental model of Rouse and Dodu to synoptic scale atmospheric inversions. He concluded that the equations governing the motion are unchanged if the density gradient between the layers is small. Then, if turbulence were generated in the lower layer of the fluid model, Ball states that an opposite dilution and inversion tendency would result. Since the model of Rouse and Dodu operated in a regime of mechanical turbulence and Ball was concerned with an atmosphere where both mechanical and thermal turbulence are present, he formed a theoretical comparison between the generation of mechanical and thermal turbulence in a deep mixing layer. The result showed that the total rate of generation of mechanical turbulence is typically an order of magnitude less than the rate of generation of thermal turbulence in this layer. In corroboration with this conclusion, Lumley and Panofsky (1964) have found that, although the rate of generation of thermal turbulence is generally much smaller than mechanical turbulence close to the surface, it can be the predominant term higher in the atmosphere; particularly in strong convective (unstable) cases and light wind conditions. In addition, Lumley and Panofsky have drawn upon the findings of other investigators (Taylor, 1952; Sheppard, 1952; Townsend, 1956; Ball, 1960), as well as their tower observations at Brookhaven, New York, to conclude that although the divergence of energy flux is small near the surface, it can be of "overwhelming importance" at higher levels. This implies that more energy is being produced at low levels than is dissipated and that this energy is transported upward, being destroyed by other processes at higher levels.

Therefore, it appears that the model of Rouse and Dodu, with the aforementioned considerations, is at least qualitatively applicable to the atmosphere. That is, we will consider a system where thermal turbulence is generated and transported vertically upward in a convection layer capped by an elevated stable layer.

In order to compare the fluidal model with actual atmospheric data collected in St. Louis, dimensional analysis via the Buckingham Π-theorem (Buckingham, 1915) of various compatible parameters were computed. First, a comparison of the density ratios in the fluid and atmospheric systems were formulated to produce a static dimensionless parameter. Rouse and Dodu ran six experiments with the ratio of the initial densities of saline (ρ) to fresh water (ρ') being:

$$\left(\frac{\rho}{\rho'}\right)_F = 1.007 \text{ to } 1.036$$

where the subscript F denotes the fluidal system. Using data from the 0700 PAC sounding taken on 23 August, the ratio of the densities of air immediately below the elevated stable layer (ρ) to that immediately above the stable layer (ρ') is:

$$\left(\frac{\rho}{\rho'}\right)_A = 1.015$$

where the subscript A denotes the atmospheric system.

A second static dimensional requirement which must be considered is geometrical similitude (Cermak et al., 1966; Hidy, 1967). Concerning geometrical similitude, Rouse and Dodu have said the following about their fluid experiment:

> "Although the functional relationships derived from the experiments are linked quantitatively with the particular geometry of the apparatus, their form should nevertheless indicate the relative roles played by the Froude and Reynolds numbers no matter what the boundary proportions might be."

Rouse and Dodu computed four dynamic dimensionless parameters for their model - a Froude number (F_F), a Reynolds number (R_F), a diffusion parameter (V_F) and a time parameter (T_F). These were expressed as:

$$F_F = \frac{\varepsilon_F}{(h^3 \Delta\gamma/\rho)^{1/2}}$$

$$R_F = \frac{\varepsilon_F}{\mu/\rho}$$

$$V_F = \frac{vh}{\varepsilon_F}$$

$$T_F = \frac{(t_o - t)\ \varepsilon_F}{h^2}$$

where:

ρ = Density of the non-turbulent (saline) layer [$M L^{-3}$]

ρ' = Density of the turbulent (non-saline) layer [$M L^{-3}$]

$\Delta\gamma = g(\rho-\rho')$ [$M L^{-2}T^{-3}$]

h = Initial thickness of the turbulent layer [L]

μ = Viscosity [$M L^{-1}T^{-1}$]

t_o = Initial time [T]

t = Terminal time [T]

v = Q/A, the derived mixing rate [$L T^{-1}$]

where:

$Q = \frac{m_e}{\rho(t-t_o)}$, the rate of efflux of entrained mass [L^3T^{-1}]

A = the area through which the mass (m_e) is entrained [L^2]

$\varepsilon_F = C_F n h^2$, the mixing coefficient [L^2T^{-1}]

where:

n = the agitator frequency [T^{-1}]

C_F = 2.5×10^{-4}, the coefficient of proportionality (Rouse, 1950).

These four dynamic dimensionless parameters are related through the functions:

$$\phi(F_F, R_F, T_F) = 0 \qquad (5.1)$$

$$\phi(V_F, R_F, T_F) = 0 \qquad (5.2)$$

$$\phi(V_F, F_F, R_F) = 0 \qquad (5.3)$$

For their six experimental runs, a plot of the data according to Equation 5.1 produced the explicit form of this equation as

$$F_F^{5/2} R_F T_F = 1.6 \times 10^{-5} \qquad (5.4)$$

However, when the data related to Equation 5.2 were plotted, no systematic trend with R_F was apparent, yielding the explicit equation

$$V_F T_F = 0.8 \qquad (5.5)$$

Rouse and Dodu concluded that,

> "The rather surprising simplicity of [Equation 5.5] actually does not indicate a lack of dependence of V_F upon F_F and R_F, but merely the fact that any change in V_F is counterbalanced by a reciprocal change in T_F."

The more pertinent function represented by Equation 5.3 was then obtained by elimination of T_F, with the result

$$\frac{V_F}{F_F^{2/5} R_F} = 5 \times 10^4 \qquad (5.6)$$

The mixing coefficient, ε_F, in the mechanically stimulated fluidal system may be expressed as K, the vertical eddy diffusivity coefficient in the thermally turbulent atmospheric system; where both coefficients are a measure of the rate of diffusion or mixing of their respective turbulent mediums and are expressed in the same units. MacCready (1970), and others have shown that the eddy diffusivity coefficient may be related in the following way:

$$K \sim \varepsilon^{1/3} \ell^{4/3} \qquad (5.7)$$

where:

ε = dissipation rate [L^2T^3]

ℓ = characteristic scale of operation [L].

To determine ℓ, one may examine Figure 5.8 and see that the entrained air reached a depth of ~300 m. Therefore, a reasonable characteristic scale of operation for this mixing process would be on the order of 300 m. In order for equation 5.7 to be valid, ε must be a measure of the dissipation rate in the "inertial subrange" considered. Statistical properties of turbulence in the inertial subrange of eddy sizes from 10 cm to 500 m may be related to ε (MacCready, 1970). The turbulence meter aboard the University of Wyoming aircraft (Appendix B) measures a quantity R [$L^{2/3}T^{-1}$] which is related to ε by the expression:

$$\varepsilon^{1/3} = R \left(\frac{\rho}{\rho_o}\right)^{-1/3}$$

where:

ρ = density at altitude [ML^{-3}]

ρ_o = density at sea level [ML^{-3}].

In the atmospheric system, the quantities utilized in the computation of the dimensionless parameters are readily transcribed from the fluidal system with the exception of v, ε_F and h.

The quantity v, the mixing rate, is actually the rate at which mass is being entrained into the turbulent layer expressed in distance per unit time. Referring back to Figure 5.8, we see that if potentially warmer air were entrained from above the

elevated stable layer shown on the 0700 PAC sounding, it would mix into the potentially cooler air immediately below this stable layer. Therefore, one would expect to see a gradient of potential temperature proceeding downward through the region of entrainment as was described in Figure 5.8. Certainly, this is what is observed in the 900-870 mb region of the 1230 PAC sounding. What was previously a layer of adiabatic temperature lapse on the morning sounding has become a near isothermal layer by 1230. The lower limit of the entrained air is at 900 mb, where it caps the mixing layer. A value for $\underline{v}$ may then be determined (for an incompressible atmosphere) by measuring the depth of the entrained air (z_e) and dividing by the elapsed time of entrainment (t_o-t). In this case, the elapsed time of entrainment is the time between the morning and midday PAC soundings. However, it must be remembered that this figure represents a maximum value since the entraining process could have occurred over a shorter time duration. The mixing rate is then:

$$v = \frac{z_e}{t_o - t} = \frac{3 \times 10^2 \text{ m}}{(5.5)(3.6 \times 10^3) \text{ sec}} =$$

$$1.5 \times 10^{-2} \text{ m sec}^{-1} .$$

Therefore, $\underline{\varepsilon}$ in equation 5.7 may be determined from aircraft data and is relative to the inertial subrange of the problem.

The atmospheric model of the entrainment process has been predicted on thermally induced turbulent energy. One may not justify the existence of turbulence at the entrainment level from eddies originating near the surface in the early morning hours. The strong surface inversion and relatively stable temperature profile up to 915 mb shown on the 0700 PAC sounding (Figure 5.2) would prevent thermally induced surface eddies from reaching the base of the elevated stable layer. In addition, lidar data (to be discussed in detail in a later section) shows that the top of the surface convection layer did not reach 900 mb until about 1100. However, early morning flights during the month of August 1971 have revealed turbulence with $\varepsilon^{1/3}$ values up to 2 cm $^{2/3}$ sec^{-1} below the base of elevated stable layers. This turbulence was typically associated with a layer of adiabatic temperature lapse which corresponded with the delineation of an elevated aerosol layer. A typical example of this turbulence phenomenon is shown for the early morning flight of 10 August 1971 in Figure 5.10. Although no early morning flight was conducted on 23 August 1971, the adiabatic profile between 915 and 870 mb suggests that this elevated turbulence may have been present. Also, an aircraft flight from 1140-1300 on 23 August 1971 showed $\varepsilon^{1/3}$ values from 2-3 cm$^{2/3}$ sec^{-1} in the deep convection layer which had formed by that time. Consequently, a value of $\varepsilon^{1/3} = 2$ cm$^{2/3}$ sec^{-1} will be used in the evaluation of the dimensionless parameters.

Hanna (1968) has empirically determined the following discrete equation for K from tower measurements in neutral and unstable conditions.

$$K = C_A \varepsilon^{1/3} k_m^{-4/3} \qquad (5.8)$$

where:

k_m = wave number (reciprocal of scale size) [L^{-1}]

$C_A = 0.055$.

This relationship is in close agreement with the work of Lumley and Panofsky (1964) and Busch and Panofsky (1968).

A value for $\underline{h}$, the initial thickness of the turbulent layer, in the atmospheric system may be assessed from the depth of the layer, beneath the elevated stable layer, in which turbulent kinetic energy may be generated. Since turbulence has been associated with layers displaying a near adiabatic lapse rate (Figure 5.10), $\underline{h}$ can be determined from Figure 5.2 as the depth of the near adiabatic layer between the top of the base of the elevated stable layer.

Computation of the dynamic dimensionless parameters for the atmosphere is now presented.

For:

$\rho = 1.045 \times 10^3$ gm m^{-3}

$\rho' = 1.030 \times 10^3$ gm m^{-3}

$g = 9.8$ m sec^{-1}

$\Delta\gamma = 147.0$ gm m^{-2} sec^{-1}

$h = 8.5 \times 10^2$ m

$\mu = 18 \times 10^{-3}$ gm m^{-1} sec^{-1}

$t - t_o = 1.98 \times 10^4$ sec

$v = 1.5 \times 10^{-2}$ m sec^{-1}

$\varepsilon^{1/3} = 2.0$ cm$^{2/3}$ sec^{-1}

$k_m^{-1} = 3 \times 10^2$ m

$C_A = 0.055$

$K = C \varepsilon^{1/3} k_m^{-4/3} = 10.25$ m^2 sec^{-1} ,

$$V_A = \frac{vh}{K} = 1.25$$

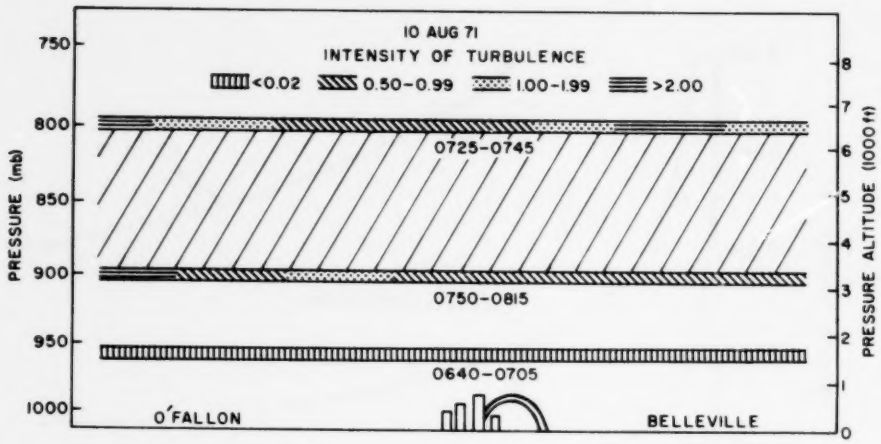

Figure 5.10. Example of early morning elevated turbulence with the 900-800 mb layer (highlighted region) being nearly adiabatic ($d\theta/dz < 2K$), while the 1000-900 mb and 800-700 mb layers showed no adiabatic character.

$$T_A = \frac{(t_o - t)K}{h^2} = 0.25$$

$$F_A = \frac{K}{(h^3 \, \Delta\gamma/\rho)^{1/2}} = 1.1 \times 10^{-3}$$

$$R_A = \frac{K}{\mu/\rho} = 5.95 \times 10^5.$$

Recalling Equation 5.5 ($V_F T_F = 0.8$) the explicit form of Equation 5.2, one can see that its counterpart in the atmospheric system is:

$$V_A T_A = 0.31 \qquad (5.9)$$

From their six runs in the fluidal experiments, Rouse and Dodu computed Froude numbers (F_F) in the range:

$$F_F = 10^{-3} \text{ to } 10^{-2}.$$

It is apparent that the Froude number in the atmospheric system ($F_A = 1.1 \times 10^{-3}$) falls in the lower portion of this range. The Reynolds number in the fluidal system (R_F) ranged from:

$$R_F = 13.1 \text{ to } 57.1.$$

In the atmospheric system, the Reynolds number (R_A) was computed to be:

$$R_A = 5.95 \times 10^5.$$

This value greatly exceeds R_F and is attributable to the greater magnitude of the atmospheric eddy diffusivity ($K = 10.25 \text{ m}^2 \text{ sec}^{-1}$), when compared with the mechanically induced mixing coefficient ($\varepsilon_F \sim 10^{-5} \text{ m}^2 \text{ sec}^{-1}$) in the fluidal system.

Since no systematic trend with R_F was found in Equation 5.5, it becomes necessary to examine the dependency of V_F on R_F and F_F, where the diffusion parameter (V_F), by its definition, is the primary factor governing the gross morphology of the entrainment process. Although equality of all the dynamic dimensionless parameters relating two systems is preferred, this is rarely possible, and it is usually necessary to maximize the similarity between those parameters which contributed most to the dynamics of the systems (Cermak et al., 1966; Daily and Harleman, 1966; Hidy, 1967).

Figure 5.11 is Rouse and Dodu's generalized plot of the diffusion parameter as it varies with the Reynolds and Froude numbers. It is readily apparent that, for relatively large (>50) values of R, the diffusion parameter tends to become highly dependent on the Froude number, but is nearly insensitive to changes in the Reynolds number.

Therefore, since the morphology of the entrainment process is governed by the diffusion parameter, and since for the calculated value of R_A the inference from Figure 5.11 is that V_A is highly dependent on F_A, it is felt that the dynamic similarity of the two systems may be evaluated by comparing F_F with F_A, along with the relationship between the time and diffusion parameters expressed in Equations 5.5 and 5.9. These comparisons and the static dimensionless parameter $(\frac{\rho}{\rho'})$, are shown in Table 5.3.

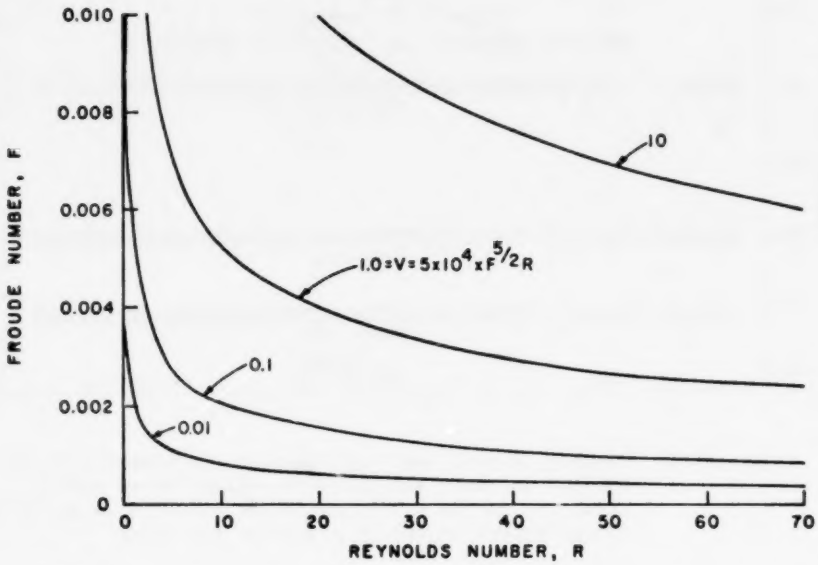

Figure 5.11. Generalized plot of the diffusion parameter (V), as a function of R and F for the fluidal system (after Rouse and Dodu, 1955).

Table 5.3. Comparison of dimensionless relationships which govern the dynamic similarity of the fluidal and atmospheric systems (Parameters are explained in the text).

Dimensionless Relationship	Value in Fluidal System	Value in Atmospheric System
$\frac{\rho}{\rho'}$	1.007 - 1.036	1.015
F	10^{-2} - 10^{-3}	1.1×10^{-3}
VT	0.80	0.31

In order to elucidate the degree of compatibility between the dimensionless parameters displayed in Table 5.3, consider a similar model - prototype comparison of dimensionless parameters conducted by Fanaki (1971). He looked at the simulation of heat flow in the lower troposphere by modeling the atmospheric system with a fluidal laboratory model. Fanaki found good agreement between the atmospheric and fluidal systems using comparable dimensionless parameters which were within an order of magnitude of their counterparts. Returning our attention to Table 5.3, it is apparent that all of the functional relationships in the atmospheric system are within an order of magnitude of their respective values in the fluidal system.

As a consequence of the similitude investigation, and with due consideration to the uncertainties present, it seems reasonable to conclude that the atmospheric system may be capable of exhibiting the entrainment phenomenon experimentally observed by Rouse and Dodu in their fluidal model.

Although the model of Rouse and Dodu may be applicable to the data of 23 August 1971, a qualitative description of the physical process which is occurring is also necessary. Consider a system where a field of turbulence is adjacent to a region of undisturbed (laminar) flow. This may be considered to be comparable to the field of turbulence below an elevated stable layer, with the

analogous laminar region existing above the turbulent field. The analogy is deemed appropriate from personal experience of aircraft flights through elevated stable layers in the St. Louis area, and is corroborated by observations from the meteorologist on board the University of Wyoming aircraft as well as data interpreted by the aircraft's turbulence meter.

In considering the fluidal system outlined above, Townsend (1956) has described a process of simple entrainment by turbulent fluid of adjacent non-turbulent fluid. He states that, broadly, the rate of entrainment is not dependent on the actual magnitude of the viscosity, but on the motion of the largest eddies. Townsend has envisaged a system where the boundary region cannot remain plane and must be continuously contorted by the various scales of the turbulent motion. Although one might not expect the boundary between regions of zero and appreciable vorticity fluctuations (non-turbulent and turbulent fields) to be a sharp division, he states that the boundary is moderately distinct, and in theory, may be treated as sharp. In discussing the transport process, Townsend says that until the ambient (non-turbulent) fluid is incorporated in the turbulent fluid, very little heat may be transferred.

One may envision a convectively turbulent field underlying a non-turbulent field, the two regions being separated by a "relatively sharp" boundary surface (the elevated stable layer). The rising turbulent eddies would then produce perturbations in the boundary surface creating a contorted wave-like surface on the scale of the larger eddies. The "valley regions" of this boundary surface would be the preferential locations for the entrainment of the non-turbulent mass (Townsend, 1956). Then, it would seem that this entrainment of non-turbulent fluid would be compensated by subsidence of air from above as dictated by mass continuity. As a result, the elevated stable layer would be capable of retaining its identity via compressional heating if the compensating subsidence brought potentially warmer air down into the region of the elevated stable layer (Ball, 1960). The net observed effect would be a warming of the air in the vicinity of the elevated stable layer.

Additional theoretical, laboratory, and field studies show supportive evidence for the entrainment scheme. Lilly (1968) presents a theoretical examination of the entrainment of warm, dry air downward through an elevated stable layer into an isentropic well-mixed layer 500-1000 m in vertical depth. Lilly formulates a relationship between entrainment of air into the turbulent region and the turbulent energy balance, and develops expressions for the minimum and maximum rates of entrainment.

$$-(\overline{w'\theta'})_h = 0 \qquad \text{(minimum)}$$

$$-(\overline{w'\theta'})_h = (\overline{w'\theta'})_o \qquad \text{(maximum)}$$

where:

$-(\overline{w'\theta'})$ = the (downward) heat flux at the top of the mixing layer,

$(w'\theta')_o$ = the (upward heat flux at the surface.

The above expression for the maximum entrainment is identical to that derived by Ball (1960). However, Deardorff et al. (1969) in their fluidal simulation of a mixing layer which was heated from below and capped by a stable layer found that the vertically integrated negative heat flux near the inversion base was <4% of the vertically integrated upward flux. Fanaki's (1971) scaled fluidal simulation of heat flow in a mixing layer suggests that (in the atmosphere) a general accumulation of warm air at the level of the inversion is a result of heat conveyed by convective columns, creating both oscillations in the inversion layer and raising its mean position.

The analyses of aircraft-supported field studies by Lenschow and Johnson (1968), Lenschow (1970, 1973) have all documented the presence of a downward flux of heat into the mixing layer. Lenchow and Johnson (1968) found that the downward flux at the inversion level (~1200 m) was 40% of the upward flux over a Wisconsin forest on a June day. The shape of the vertical heat flux profile was similar to Ball's (1960) model, but inspection of the energy-budget showed no evidence of the strong upward energy transport to the inversion level required by the model (for eddy wavelengths up to the instrument's maximum measurable value of 1.3 km). Aircraft measurements over Lake Michigan in winter by Lenschow (1973) show that the downward flux at inversion level (~800 m) was <8% of the upward surface flux. On one of his case studies, he calculated an entrainment rate (velocity) of 1×10^{-2} m sec^{-1}, in good agreement with the 23 August 1971 entrainment rate of 1.5×10^{-2} m sec^{-1} calculated in our work.

The investigations mentioned above suggest that the elevated entrainment process is active in the atmosphere, and that evaluation of its magnitude is contingent on the underlying surface and meteorological

conditions. Our 23 August 1971 case injects an additional variable; i.e., the presence of elevated turbulence associated with an elevated aerosol layer. This localized source of turbulent kinetic energy, generated at the level of the elevated stable layer, may preempt the demand on the vertical transport of surface generated thermal kinetic energy, providing a greater driving force in the elevated entrainment process.

Next, it seems reasonable to ask why the entrainment process was detectable at PAC and not ARC on 23 August 1971. Since both sites recorded elevated stable layers of approximately the same intensity and elevation on the morning soundings, it would appear that this factor is not singly determinate upon the entrainment process. Another necessary ingredient in this process is the existence of turbulent kinetic energy immediately below the elevated stable layer. Examination of the 0700 ARC sounding (see Figure 5.1) shows a less than adiabatic temperature profile below the base of the stable layer at 860 mb. There is ∿2K ascendent of potential temperature at ARC from 935-860 mb, while the 0700 PAC sounding shows a zero ascendent from 915-870 mb. As previously mentioned, elevated early morning turbulence had been typically found to be associated with an adiabatic (and in some instances superadiabatic) temperature lapse rate in conjunction with the presence of an elevated aerosol layer. Therefore, it is possible that the absence of early morning elevated turbulence prohibited the entrainment process from operating over ARC.

A second possibility would be that the entraining process did occur over ARC between 0700 and 1230, but that it was undetectable, or masked by the time the 1230 sounding was recorded. A comparison of the 1230 ARC and PAC thermal profiles in Figure 5.12, and the heating profiles in Figure 5.4, shows that although PAC received more relative heating in the 900-850 mb layer, it still displayed a mean potential temperature of almost 2K less than ARC in that layer. Comparing the thermal profiles from 1000-900 mb, one finds that ARC was nearly 3K warmer than PAC through this layer, even though the respective surface temperatures were only 1K apart. Therefore, the strong degree of heating in the mixing layer below 870 mb at ARC may have been sufficient to mask any elevated warming due to entrainment prior to the 1230 sounding. This is a case where the magnitude of the surface heat island is small, but the relative differential through the vertical from 1000-850 mb between ARC and PAC is quite distinctive. An explanation of the formation of this anomaly is suggested later in this paper.

If the magnitude of the relatively increased heating in the deep mixing layer over ARC was sufficient to mask the elevated entrainment process, then an explanation must still be sought for absence of an elevated stable layer on the 1230 ARC sounding. Since a deep mixing layer existed on the 1230 ARC sounding, then it is reasonable to assume that this convection layer may have existed at some earlier time when the elevated stable layer shown on the 0700 ARC sounding was still present. Now, if the entrainment process described in the atmospheric model is capable of proceeding via turbulent kinetic energy generated in a deep mixing layer, as well as the previously discussed early morning elevated turbulence, then the destruction of the elevated stable layer over ARC deserves further scrutiny.

The entrainment process was assumed to operate on a characteristic scale length compatible with the depth of the entrained air (∿300 m). However, thermals originating at the surface in the deep mixing layer shown on the 1230 ARC sounding could have eddy sizes as large as 1200 m (the depth of the mixing layer). For the entrainment process to occur in the scale regime dictated by the atmospheric model, then these large thermal eddies must be broken down into smaller eddies. Therefore, two possibilities exist. Either the entrainment process may not occur when stimulated by large thermal eddies, or these eddies produce smaller scale eddies which are compatible with the scale of the problem. A method whereby large thermal eddies may be broken into smaller eddies below the base of an elevated stable layer is suggested in the following paragraph.

Various investigations have examined the horizontal diameter of thermals [see Warner and Telford (1967) for a discussion of the literature; also Lenschow (1970)]. These findings show that thermals originating at the surface have a typical diameter of 200-300 m, and may maintain this diameter as they proceed upward, or spread out to as much as 900 m at an altitude of 600 m. Now consider a buoyant thermal as it rises vertically and impacts an elevated stable layer. A laboratory simulation has shown that the thermal will subsequently diverge horizontally at the base of the elevated stable layer (Fanaki, 1971). As this occurs, a layer of turbulent air (probably about one-half the thermal diameter) will spread out beneath the elevated stable layer. This layer would presumably contain turbulent eddies on the order of one-half the thermal diameter and smaller, compatible with the characteristic scale size in the atmospheric model of the entrainment process.

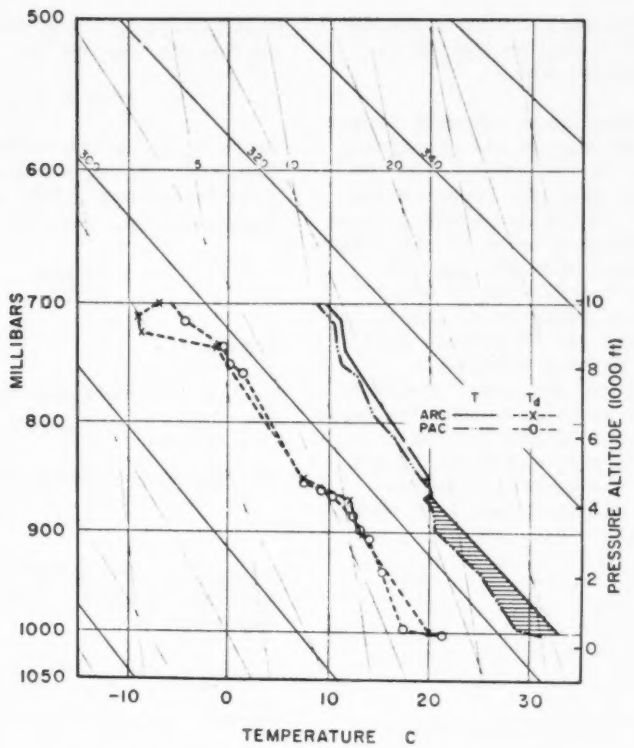

Figure 5.12. ARC and PAC 1230 radiosonde observations highlighting the vertical heat island.

If this method is capable of producing a characteristic scale size agreeable with the atmospheric entrainment model, a consideration of the lack of elevated warming over ARC is warranted. In a deep mixing layer, large thermals with eddy size scales which reach an order of the depth of the mixing layer are probably present, and would continuously transfer heat throughout the layer as they rise and descend. These eddies would tend to redistribute any elevated warming connected with the entraining process throughout the entire mixing layer, or at least elongate the downward extent of the elevated heating profile. Indeed, Warner and Telford (1967) have found that $d\theta/dt$ in a mixing (convection) layer is usually constant with height, implying that heating at the surface (or possibly from aloft) tends to be distributed uniformly in the mixing layer; and is in general agreement with the predictions of Malkus (1954), the findings of Thomas and Townsend (1957), and the experiments of Webb (1958).

The foregoing considerations suggest two implications of the elevated entrainment process in the atmosphere. First, the process probably operates with a characteristic eddy scale size of a few hundred meters or less. Second, if the process is capable of functioning in a deep convection layer via the horizontal divergence of ascending thermals beneath an elevated stable layer, the elevated warming may be redistributed downward through the convection layer by the motion of large convective eddies. This compensating motion may render the elevated entrainment process undetectable, or at least mask its localized effect. The second implication is surely a function of several unknown parameters (i.e., accurate thermal properties, wind shear, vertical heat flux, turbulent dissipation) which inhibit the prediction of its overall effect under various meteorological regimes.

Another point to be considered is that Rouse and Dodu saw a migration of the interface toward the non-turbulent layer. In the atmospheric system, this would correspond to a rising of the elevated stable layer. This seems intuitively appropriate since mass entrained into the turbulent layer would facilitate a rising of the interface by virtue of the continuity equation. The base of the elevated stable layer on the 0700 PAC sounding is at 870 mb. At 1230, a stable layer of nearly the same intensity is again found at 870 mb, with the depth of the entrained air extending 30 mb below it. If mass continuity

holds, then one would expect to see a rising of the elevated stable layer in accordance with the rate of entrained air.

However, if a broad scale synoptic divergence of the same magnitude as the entraining process was occurring in the layer below the elevated stable layer, then the compensating motion in the opposite direction would account for the apparent stationary level of the stable layer. The rate of entrained air was previously calculated as $v = 1.5 \times 10^{-2}$ m sec^{-1}. In order to compute the synoptic vertical velocity in this layer, the 0700 winds from the National Weather Service radiosonde soundings at PIA, SLO and UMN were considered. These stations form a triangle around St. Louis (Figure 5.13) and create an ideal situation for the calculation of horizontal divergence (or convergence) via the method of Bellamy (1949). The "layer technique" was used where the horizontal divergence was computed from the mean wind in the 1000-940 mb layer, and again from 940-970 mb. These values were found to be 9×10^{-6} sec^{-1} and 7×10^{-6} sec^{-1}, respectively. The resulting vertical velocity at 870 mb may then be found by the familiar kinematic method.

First, consider the continuity equation in the form:

$$\nabla \cdot V + \frac{1}{\rho} \frac{d\rho}{dt} = 0.$$

Multiplying by ρ and expanding the total derivative results in:

$$\rho \nabla \cdot v + \frac{\partial \rho}{\partial} + V_H \cdot \nabla \rho = 0$$

where $V_H \cdot \nabla \rho$ is the horizontal advection of density. Making the assumption the $V_H \cdot \nabla \rho + \frac{\partial \rho}{\partial} = 0$ (Bellamy, 1949) and expanding $\rho \nabla . v$ into horizontal and vertical components gives:

$$\frac{\partial (\rho w)}{\partial Z} = -\rho \nabla \cdot V_H$$

where:

w = vertical velocity [LT^{-1}],

$\nabla . V_H$ = horizontal divergence [T^{-1}].

In finite difference form this becomes:

$$\nabla \rho w = -\rho \nabla \cdot V_H \Delta z$$

where Δz = the thickness of the layer considered. From z = a to z = b, this may be expressed as:

$$(\rho w)_a = (\rho w)_b - (\bar{\rho}_{ab})(Div_{b-a})(z_b - z_a) \quad (5.10)$$

where:

$(\rho w)_b$ = density times vertical velocity at the top of the layer [ML^{-3}],

$(\rho w)_a$ = density times vertical velocity at the bottom of the layer [ML^{-3}],

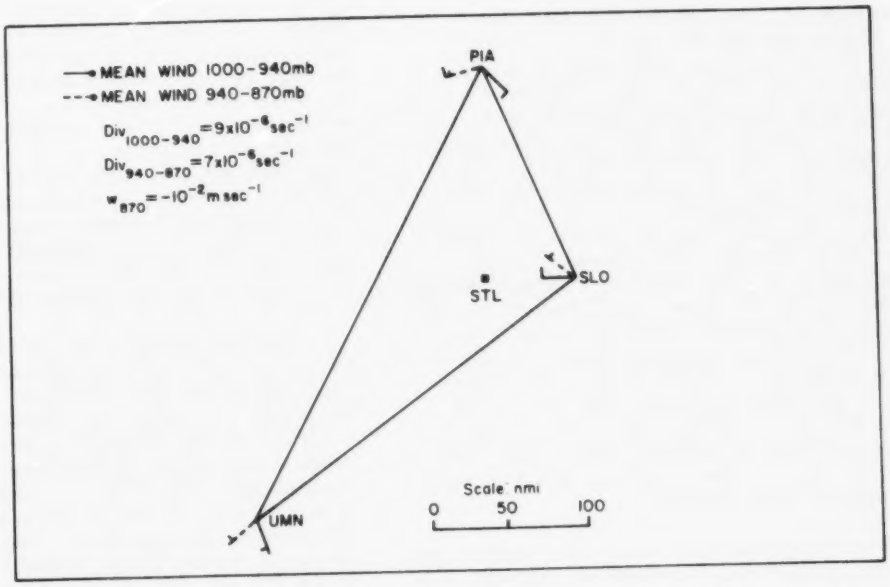

Figure 5.13. Data used in the calculation of synoptic scale vertical velocity at 870 mb (w_{870}), where a full wind barb equals 10 knots.

$\bar{\rho}_{ab}$ = $1/2(\rho_a + \rho_b)$, the mean density in the layer $[ML^{-3}]$,

Div_{b-a} = the horizontal divergence in the layer $[T^{-1}]$.

Making the customary assumption that $(\rho w)_a = 0$ at the surface, the vertical velocity at 940 mb is $w = -5.4 \times 10^{-3}$ m sec^{-1}. Using this value for w_a in equation 5.10 results in a vertical velocity at 870 mb of $w = -10^{-2}$ m sec^{-1}. This figure corresponds well with the rate of entrained air, $v = 1.5 \times 10^{-2}$ m sec^{-1}, when one considers the magnitude of observational uncertainties. Therefore, it seems reasonable that the theoretical rising of the elevated stable layer may have been compensated by synoptic divergence, suggesting an explanation for the absence of any observed upward migration.

Radiative Effects of Aerosol Layers on Vertical Temperature Structure. As previously mentioned in Section II, various investigators have seen that aerosol (haze or mixing) layers are often capped by an elevated stable layer (which in some cases exists as a temperature inversion). Examination of lidar data will show that the stable layer generally forms through the nocturnal hours at the top of the existing aerosol layer from the previous day. Comparison of lidar and temperature sounding data has revealed the presence of an elevated stable layer capping an aerosol layer on all mornings when comparable data were available (12, 13, 18, 19, 24, 25 August 1971).

The SRI/EPA Mark VII Lidar Unit ran continuously at a location 0.25 n mi north of ARC from 1000 23 August to 2050 24 August 1971, the only period when the lidar unit was operating during nocturnal hours. It is felt that an examination of a portion of these data relating to the formation of elevated stable layers and associated aerosol layers is pertinent. Figure 5.14 is a reproduction of the lidar data from 2155 23 August to 0700 24 August 1971, the intensity of the profile corresponding to the intensity of the reflected pulses. The intense reflection at the top of the aerosol layer from 2155-2205 is a reflection from cloud base, the last

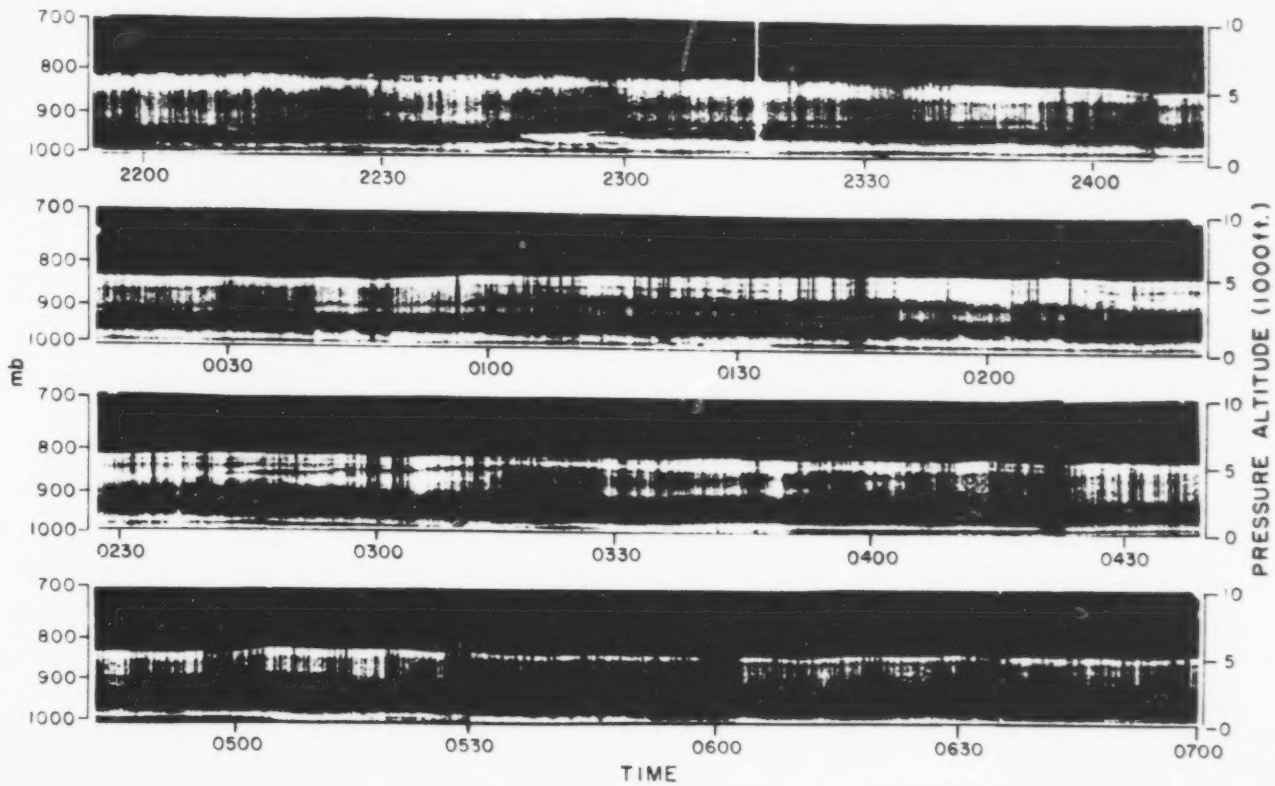

Figure 5.14. Height-time cross section of the aerosol structure from 2155 on 23 August to 0700 on 24 August 1971. (After Uthe and Kealoha, 1972)

remaining convective activity of the day. The presence of these clouds implies a lack of any elevated stable layer at that time which would inhibit convective cloud formation. During the nocturnal hours, two distinct aerosol layers are delineated; one which extends from the surface upwards a depth of a few millibars, and an elevated aerosol layer from about 920-850 mb. The elevated aerosol layer represents the bulk of the previous day's mixing layer with its upper extremity approximately corresponding to the maximum elevation of that layer. A Schematic representation of the 0700 aerosol profile superimposed on the 0700 24 August 1971 ARC sounding is shown in Figure 5.15. One immediately notices that the upper extremity of the elevated aerosol layer corresponds directly with the level of the elevated stable layer; and that the mean temperature profile through the elevated aerosol layer is nearly adiabatic, being superadiabatic from 915-880 mb. Below the elevated aerosol layer a stable temperature profile exists, which corresponds to an absence of pulse reflections.

Since an early morning elevated stable layer seems to be associated with the presence of an aerosol layer, an investigation into a possible mechanism will be considered. Atwater (1970) developed a numerical model which examined the significance of the radiative effects of pollutants on urban temperature profiles. His model also utilized the corroborative empirical data of Davis (1965). Atwater found that aerosol layers may have cooling rates due to radiative loss which exceed that attributed to water vapor (~4.5 precipitable centimeters), depending on their absorption coefficient (B_a). For $B_a > 0.1$ km^{-1}, it was found that the cooling rate of an aerosol layer will exceed that due to water vapor. A reproduction of Atwater's data for $B_a = 0.1$ km^{-1} and $B_a = 1.0$ km^{-1} in Figure 5.16 shows that these cooling rates may reach appreciable magnitudes. Moreover, he found that the cooling rate of an aerosol layer is proportional to the concentration of aerosols, and that the maximum decrease in temperature occurs within the aerosol layer, gradually extending through a deeper layer. This last point may be illustrated by examination of the infrared cooling profile at the left side of Figure 5.17 (after Atwater, 1970). Atwater concluded that,

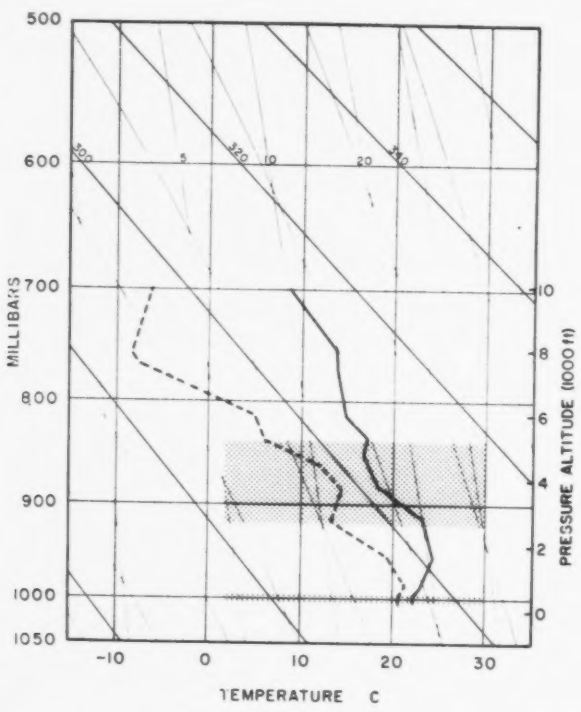

Figure 5.15. ARC radiosonde observation recorded at 0700 on 24 August 1971 and a schematic representation of the 0700 aerosol profile as observed by lidar.

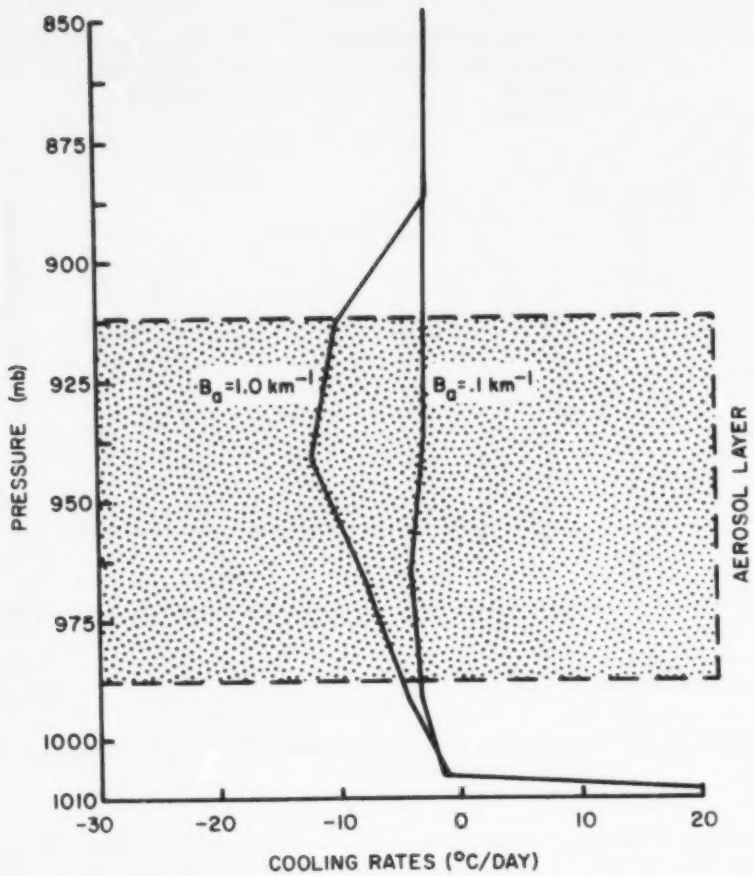

Figure 5.16. Infrared cooling rates from gaseous and particulate absorption for the Davis (1965) night sounding (after Atwater, 1970).

> "In general, differential cooling associated with the polluted layer results in cooler temperatures within the polluted layer. A more stable layer, or an inversion, forms above the polluted layer."

The numerical model also showed that when aerosols were absent, no elevated stable layer formed.

Therefore, radiative cooling of an elevated aerosol layer may indeed be a process capable of creating an elevated stable layer. To determine that the aerosol layer did cool from sunset 23 August to sunrise 24 August 1971, consider data shown in Figure 5.18. The figure again shows a schematic of 0700 lidar and ARC sounding data along with the temperature profile recorded by the aircraft on descent from 5000 ft MSL between BLV and Alton from 1852-1903 23 August 1971. Notice that the potential temperature from 920-850 mb shows a constant value of about θ = 306K, while the surface inversion has already begun to form below 920 mb. The 920-850 mb region on the 0700 24 August 1971 sounding shows a mean value of $\bar{\theta}$ = 303K, a cooling of 3K in 12 hours. Another salient feature of Figure 5.18 is that the minimum potential temperature (θ = 302K) in the 920-850 mb layer on the morning sounding is found near the middle of this layer, in agreement with Atwater's predicted cooling profile in Figure 5.17.

If the creation of an elevated stable layer associated with an elevated aerosol layer may be attributed to nocturnal infrared cooling, then the fate of these two phenomena after sunrise deserves examination. Figure 5.19 shows the distribution of aerosols from 0700-1230 24 August 1971. The top of the elevated aerosol layer has risen approximately 60 mb while the aerosol layer itself has

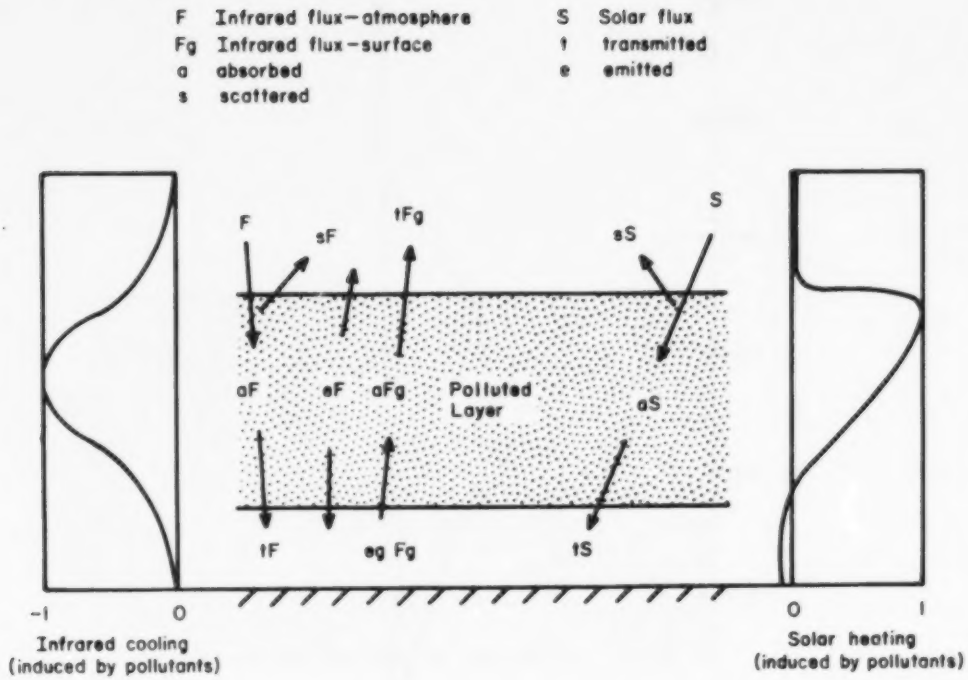

Figure 5.17. Changes in radiation caused by the presence of a polluted layer (After Atwater, 1970).

gradually decreased in intensity. Meanwhile, the surface mixing (convection or aerosol) layer is steadily rising as solar insolation increases. The schematic of the lidar picture superimposed over the 1230 ARC sounding in Figure 5.20 again shows that the top of the elevated aerosol layer is in close proximity to the level of an elevated stable layer. From 915-770 mb, a conditionally unstable temperature profile exists while a near adiabatic lapse is observed from 1000-915 mb which corresponds with the depth of the surface mixing layer. The major portion of the warming in the 915-770 mb layer has occurred in the area immediately below the level of the previously existing elevated stable layer recorded on the 0700 sounding. This brings to mind the skewed hour-glass heating profile observed on 23 August 1971 (Figure 5.4), and the possibility of elevated warming due to the previously described entrainment process. However, another possibility is the heating of the elevated aerosol layer from (low zenith angle) solar insolation. Atwater found that appreciable heating rates may occur in the upper portion of an aerosol layer. His numerical model predicts a heating profile shown on the right side of Figure 5.17 which is compatible with both the observed heating structure and that of the entrainment process (Figure 5.8).

Figure 5.21 shows the aerosol distribution from 1230-1700 on 24 August 1971. Note that the top of the elevated aerosol layer lowers between 1230-1315 while the surface convection layer is still rising. By 1400 the two aerosol layers have become one, but there is virtually no increase in the depth of this combined aerosol layer for more than two hours until 1610, during a period when solar insolation is near a maximum and surface observations at Lambert Field reported clear skies. This suggests that the stable layer which is shown capping the elevated aerosol layer at 0700 and 1230 is still present from 1400-1610 and is inhibiting free convection. At 1610, the top of the combined aerosol layer rises abruptly and maintains a height of about 780 mb. The STL observer reported cumulus formation after 1600.

The analysis of lidar and sounding data from 2155 23 August to 1700 24 August 1971 suggests the following general conclusions:

1. Elevated stable layers seem to form at the top of an aerosol layer through infrared cooling in the aerosol layer during nocturnal hours.

2. The elevated stable layer and associated aerosol layer may augment the

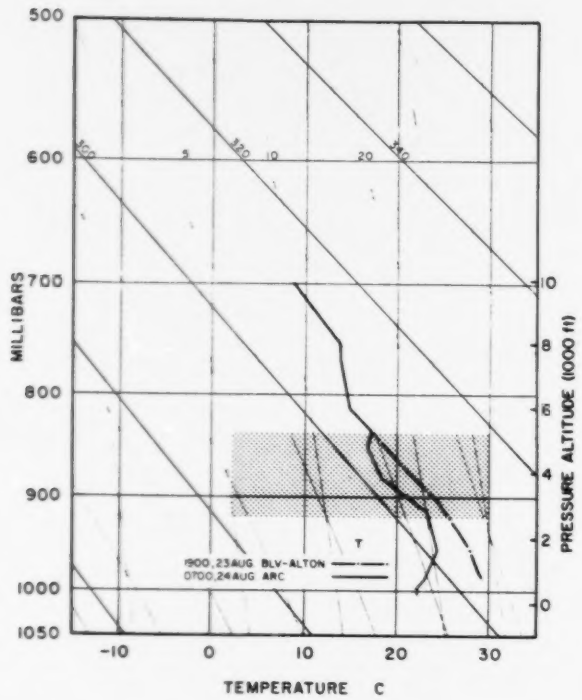

Figure 5.18. Cooling of the 920-850 mb layer in the ARC vicinity from 1900 on 23 August and 0700 on 24 August 1971. The dot pattern is a schematic representation of the aerosol layer at 0700 on 24 August as observed by lidar.

vertical temperature structure through the aerosol layer during the daylight hours.

3. This augmentation of the temperature structure could be attributed to radiational heating of the aerosol layer and/or the elevated entrainment process; these processes have the compound effect of warming the upper portion of the aerosol layer.

With these considerations in mind, attention will now be focused on the available lidar and sounding data for the daytime hours of 23 August 1971. The 0700 23 August 1971 ARC sounding (Figure 5.22) shows an elevated stable layer based at 860 mb. The lidar unit did not operate until 1000 on that day; the aerosol distribution from 1000-1230 is displayed in Figure 5.23. At 1000 the top of the upper aerosol layer is shown at about 880 mb. If the elevated stable layer on the 0700 sounding capped the upper aerosol layer at that time, then some process has occurred which reduced the aerosol intensity in the 880-860 mb region between 0700-1000. The reflection of the lidar signal is a function of particle size as well as concentration. Hygroscopic (haze) particles in the aerosol layer will shrink with decreasing relative humidity since they are in equilibrium with their environment. Therefore a decrease in relative humidity will reduce the intensity of the returning lidar signal providing the concentration of particles remains constant (Uthe and Kealoha, 1972). A decrease in relative humidity is facilitated by increasing temperature and decreasing water vapor content. If an aerosol layer did exist below the elevated stable layer at 0700, warming of the upper portion of this layer due to low zenith angle solar insolation and/or via the elevated entrainment process would result in a decrease in lidar reflectivity. Examination of the 0700 and 1230 ARC dew point traces in Figure 5.22 shows that the entire layer below 860 mb decreased in water vapor content approximately 2 gm kg^{-1}. Winds were from the southwest and advection from the PAC vicinity cannot account for this magnitude of change. The only source of substantially

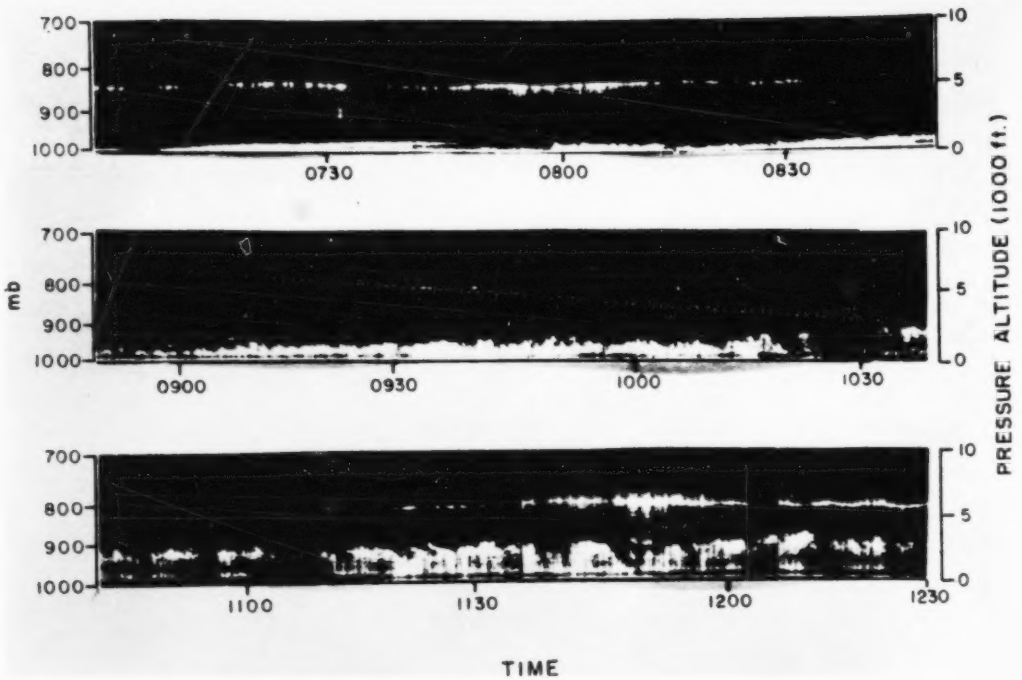

Figure 5.19. Height-time cross section of the aerosol structure from 0700-1230 on 24 August 1971. (After Uthe and Kealoha, 1972).

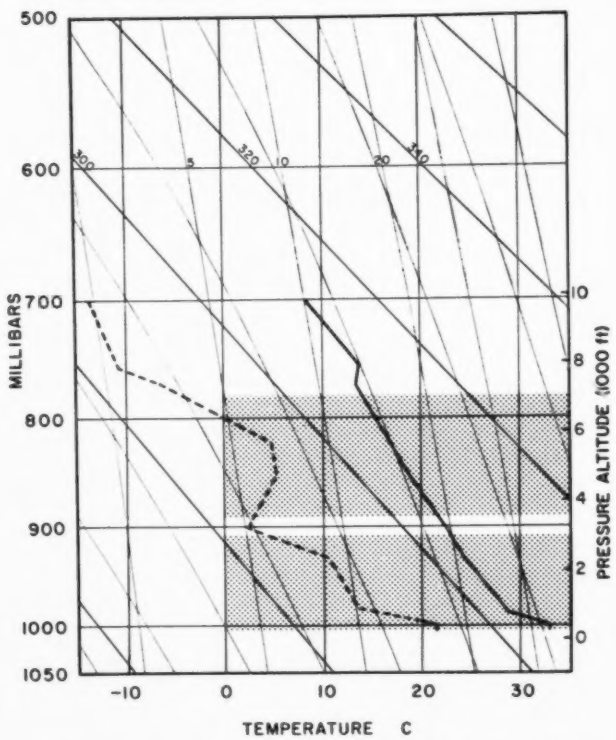

Figure 5.20. ARC radiosonde observation recorded at 1230 on 24 August 1971 and a schematic representation of the 1230 aerosol profile as observed by lidar.

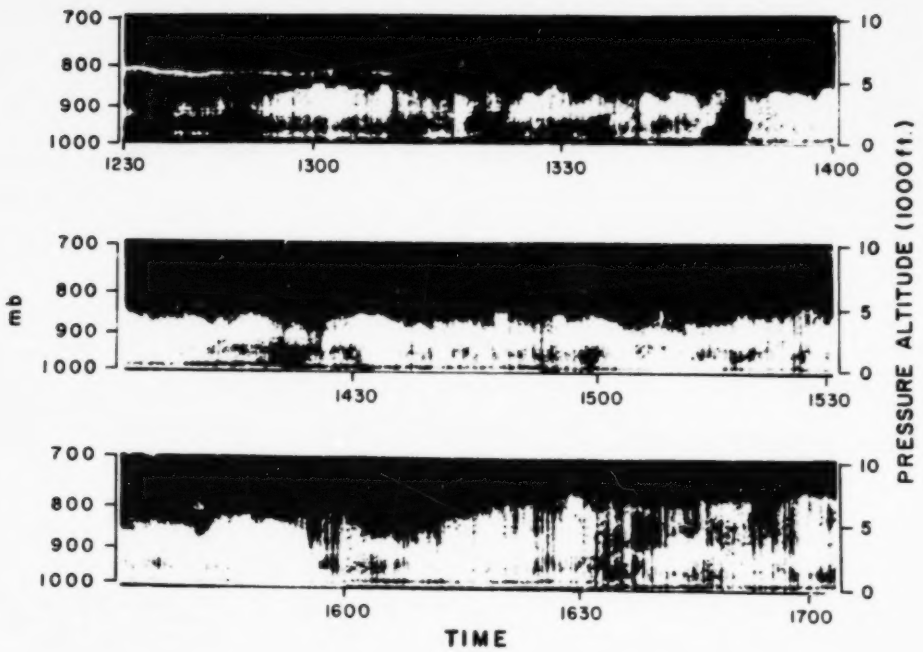

Figure 5.21. Height-time cross section of the aerosol structure from 1230-1700 on 24 August 1971. (After Uthe and Kealoha, 1972).

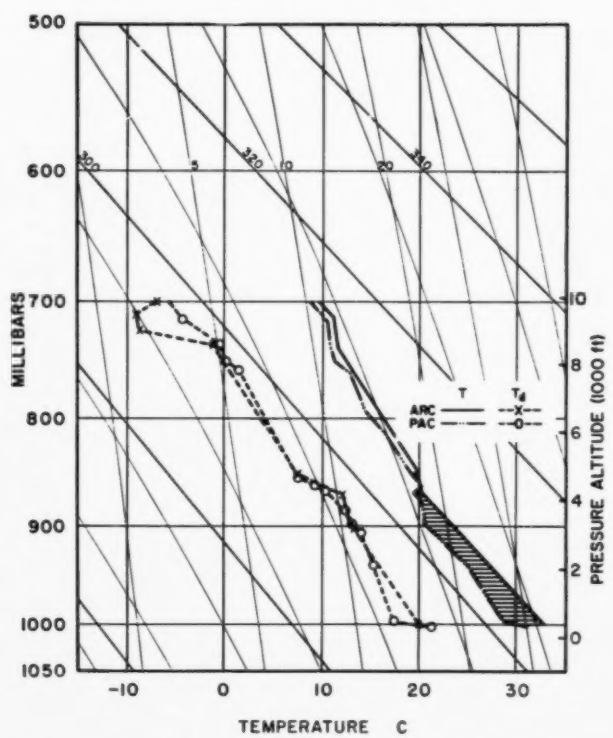

Figure 5.22. ARC radiosonde observations recorded at 0700 and 1230 on 23 August 1971.

drier air is above the elevated stable layer, this air being on the order of 5 gm kg^{-1} drier than the air immediately below the elevated stable layer. Therefore, a plausible mechanism which would decrease the lidar intensity in the 880-860 mb region is the entrainment of warmer drier air from above the elevated stable layer. If this process occurred, it may also be reflected in the drying of the entire mixing layer by 1230.

At 1000, lidar data from Figure 5.23 indicates that the top of the surface aerosol layer has already reached a height of 940 mb, and by 1055, the top of the two aerosol layers are congruent at about 915 mb. The depth of this combined aerosol (mixing) layer then remains constant for only 20 min until 1120. Therefore, if an elevated stable layer capped the mixing layer at 1100, it was probably weak since it did not substantially inhibit free convection. From 1130-1230 the mixing layer rose to a height of 830 mb and showed evidence of vigorous convection (instability) as reflected in its irregular top surface (Uthe and Kealoha, 1972). The 1230 ARC sounding in Figure 5.22 shows that the temperature lapse rate in the mixing layer is strictly adiabatic. Above this level, a 20-mb layer of conditionally unstable air may be the remains of the elevated stable layer at 0700. The existence of this 'weak' conditionally unstable layer then justifies the very brief inhibition to free convection from 1100-1120.

The depth of the mixing layer rose steadily to a height of approximately 830 mb (5500 ft MSL) from 1120-1245 (Figures 5.23 and 5.24) when a large signal was returned from the top of the aerosol layer indicating the lidar had detected a convective cloud (Uthe and Kealoha, 1972). From 1245 to 1700, the height of the mixing layer remained essentially constant while the lidar gave evidence of numerous convective clouds with bases at 5500-6000 ft MSL. The detection of these convective clouds by the lidar unit is in agreement with the observed convective activity described in Section 4.2.

The lidar unit was stationary on 23 August 1971 and there are no aerosol distributions for the PAC vicinity. However, the formation of convective activity at ARC has been shown to depend on the establishment of a deep adiabatic mixing layer extending to cloud base, and the absence of an elevated stable layer at the top of this mixing layer. Recalling the heating profiles in Figure 5.4 shows that PAC did not meet the above requirements. The elevated warming at PAC could be a reflection of either radiative heating or elevated entrainment. The strictly adiabatic temperature profile from 915-870 mb on the 0700 PAC sounding could imply a more relatively intense aerosol layer or region of greater turbulence, both of which would increase the elevated heating trend. In conjunction with (and possibly a result of) the elevated heating at PAC, the relatively lesser degree of heating in the 1000-900 mb region helped to inhibit the formation of a deep adiabatic mixing layer extending to cloud base.

The difference in vertical heating profiles observed at ARC and PAC may be attributable to four factors.

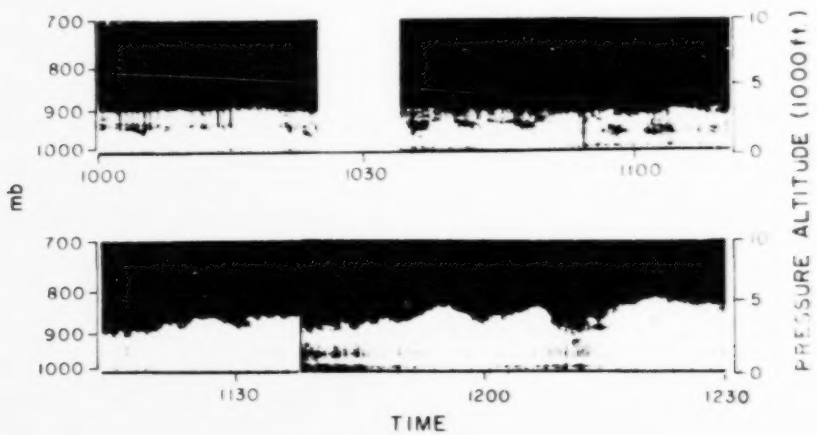

Figure 5.23. Height-time cross section of the aerosol structure from 1000-1230 on 23 August 1971. (After Uthe and Kealoha, 1972).

Reproduced from best available copy.

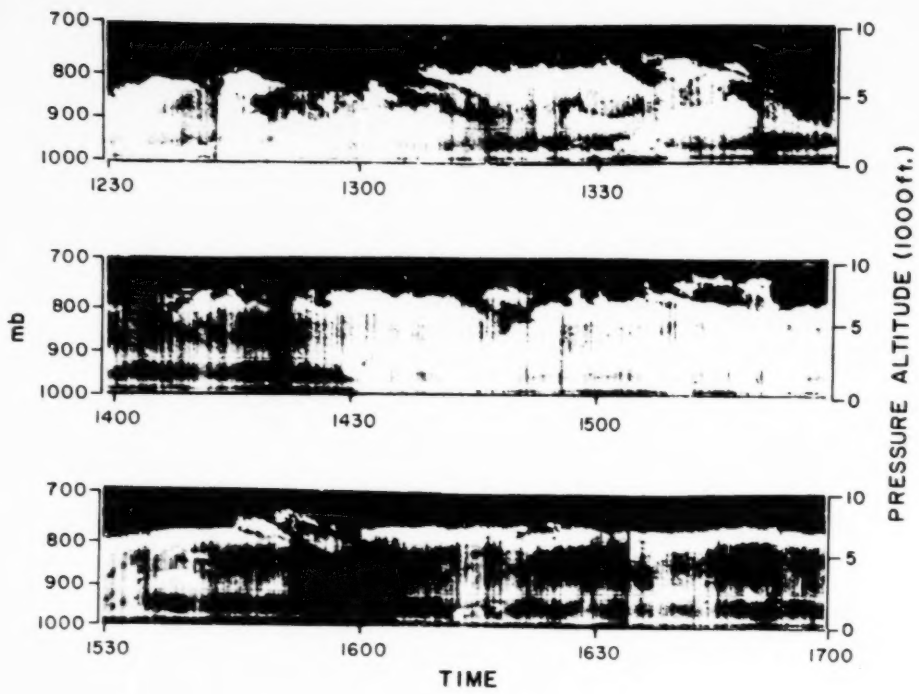

Figure 5.24. Height-time cross section of the aerosol structure from 1230-1700 on 23 August 1971. (After Uthe and Kealoha).

1. The morning ARC sounding was already ∿1K warmer than PAC in the 1000-850 mb layer.

2. The strong surface inversion at PAC took longer to "break" (see Section 4.2) than ARC and inhibited deep convective mixing.

3. The morning PAC sounding was saturated near the surface, causing a portion of the incoming solar radiation to be expended in the evaporation of liquid water, while another portion was probably reflected back into the atmosphere due to the presence of the fog deck.

4. The fact that the morning PAC sounding showed a more adiabatic temperature character than ARC below the elevated stable layer suggested that the elevated aerosol layer over PAC may have been more intense, therefore absorbing and/or backscattering a greater amount of the incoming solar radiation.

As a consequence of the analyses of lidar data, one could imply that the observed elevated heating trend at PAC on 23 August 1971 is related to the vertical and spatial aerosol structure. It should also be noted that this postulated contribution to elevated heating may be compounded with the effect of the elevated entrainment process in that

1. both contributions are associated with a layer of air where the temperature lapse rate approaches adiabatic, capped by an elevated stable layer, and

2. the realizable heating is found in the upper portion of the (adiabatic) layer just beneath the elevated stable layer.

Furthermore, the difference in vertical temperature profiles at ARC and PAC which governed the location of convective activity on 23 August 1971 appears to be an effect of the elevated entrainment process and/or a function of aerosol structure.

5.3 13 August 1971

Elevated Heating Profiles. In this case study, an analysis of the heating profile is shown in Figure 5.25 for the 0700 and 1530 PAC soundings, and compared with the heating profile between the 0700 ARC and 1600 TOY soundings. Again we find the "skewed hourglass" profile on one of the heating profiles;

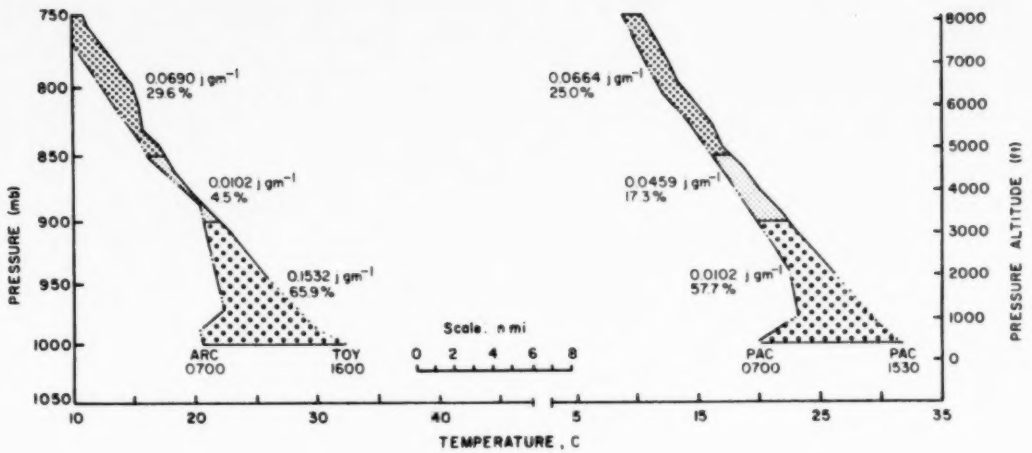

Figure 5.25. Heating profiles from 0700-1230 at PAC and ARC on 13 August 1971.

however, in this case it is located over the ARC-TOY area while PAC showed relatively uniform warming. As was the case in the 23 August study, the skewed hour glass profile is located in nearest proximity to the area of inhibited convective cloud activity. Examination of the heating profiles for the three surrounding NWS radiosonde sites (UMN, SLO, PIA), revealed that the elevated heating trend at ARC-TOY appeared to be a unique occurrence in that it was not observed at any of these surrounding NWS radiosonde sites, or at PAC.

Advection in the Vicinity of an Elevated Stable Layer. An examination of the prevailing wind field in the manner used in the 23 August case study suggested that neither synoptic nor meso-scale advective processes could account for the observed elevated heating over ARC-TOY, and that the St. Louis urban area may have been capable of selectively modifying vertical temperature structure.

Examination of the Processes Associated with Elevated Heating. Since horizontal advection is again incapable of explaining the convectively inhibiting elevated warming over ARC-TOY, attention will now be focused on the processes associated with the selected elevated warming previously discussed in Section 5.2. This discussion suggested that nocturnal radiative cooling was responsible for the formation of an elevated stable layer at the top of an aerosol layer.

Further supporting evidence may be gleaned from the 12 August 1971 data of Spangler and the previously mentioned work of Atwater (1970). Spangler found Aitken nuclei counts (an indication of the total particulate matter in the air) within the elevated stable layer to be an order of magnitude greater at ARC than PAC at 1930 12 August 1971. Atwater found that the rate of infrared cooling is proportional to aerosol concentration. At 1930 on 12 August 1971, aircraft soundings showed that the ARC-TOY area was about 1.5K warmer than PAC through the mixing layer. Since there was only a few tenths difference in potential temperature between the 0700 13 August 1971 ARC and PAC soundings in the 100 mb layer below the altostratus deck (see Section 4.3), it is apparent that, during the nocturnal hours, the aerosol layer over PAC did experience a greater degree of cooling ($\sim$1.5K) than did the aerosol layer over ARC-TOY. The culmination of these data suggests that the elevated stable layer over PAC probably displayed a weaker character than that observed at ARC.

Similar to the elevated heating profile at PAC on 23 August 1971, one may notice that the elevated heating at ARC on 13 August 1971 occurred chiefly in the region immediately below the elevated stable layer (the upper portion of the aerosol layer).

An analysis of the broad scale regional synoptic divergence, same as that exercised in the 23 August case study, revealed a computed subsidence of the elevated stable layer of about 60 mb from 0700-1600 (and continuous past 1900). The mean elevation of the elevated stable layer subsided 65 mb in this time period, in good agreement with the computed subsidence. If the synoptic scale divergence pattern was acting on the St. Louis

area, it is reasonable to assume that PAC was also subjected to its dynamic influence. However, if the elevated stable layer over PAC were weaker than that over ARC-TOY (as suggested above), such that there was no elevated heating via entrainment and/or aerosol heating, one would not expect to see a "skewed hour glass" profile. The fact that PAC warmed uniformly between 0700 and 1530 (Figure 5.25) supports this rationale and implies that the elevated stable layer over PAC was extremely weak.

Since simple subsidence of the elevated stable layer over ARC would not alter the character of $\frac{d\theta}{dz}$ through that layer, it was suggested that aerosol heating and/or entrainment of potentially warmer air from above the stable layer generated the observed elevated heating profile. The aerosol layer present during the morning hours over ARC on 13 August 1971 was considerably deeper than that observed on 23 August 1971. Therefore, warming of the top portion of this aerosol layer on 13 August 1971 due to either entrainment or heating from solar insolation would tend to be redistributed downward through a greater depth than that observed on 23 August 1971. It is felt that one or both of these processes helped contribute to the observed heating profile over ARC-TOY on 13 August 1971.

To substantiate this, consider Figure 5.26 which shows smoothed values of $\varepsilon^{1/3}$ ($cm^{2/3}$ sec^{-1}) plotted against height as recorded on two ascending spiral soundings taken at PAC (1530) and TOY (1600), and the following discussion of turbulent kinetic energy.

In the absence of convergence of the turbulent flux of kinetic energy, it is known (Lumley and Panofsky, 1964) that ε is related to the generation of turbulent kinetic energy by:

$$\varepsilon = \frac{gH}{C_p \rho T} + \frac{\tau \partial \bar{v}}{\rho \partial z} \qquad (5.12)$$

where H is the upward vertical flux of heat, τ is the shearing stress, $\bar{v}$ is the mean horizontal wind component, and the other parameters have their usual meaning. Since we are concerned with the generation of turbulent kinetic energy from thermal (buoyancy)

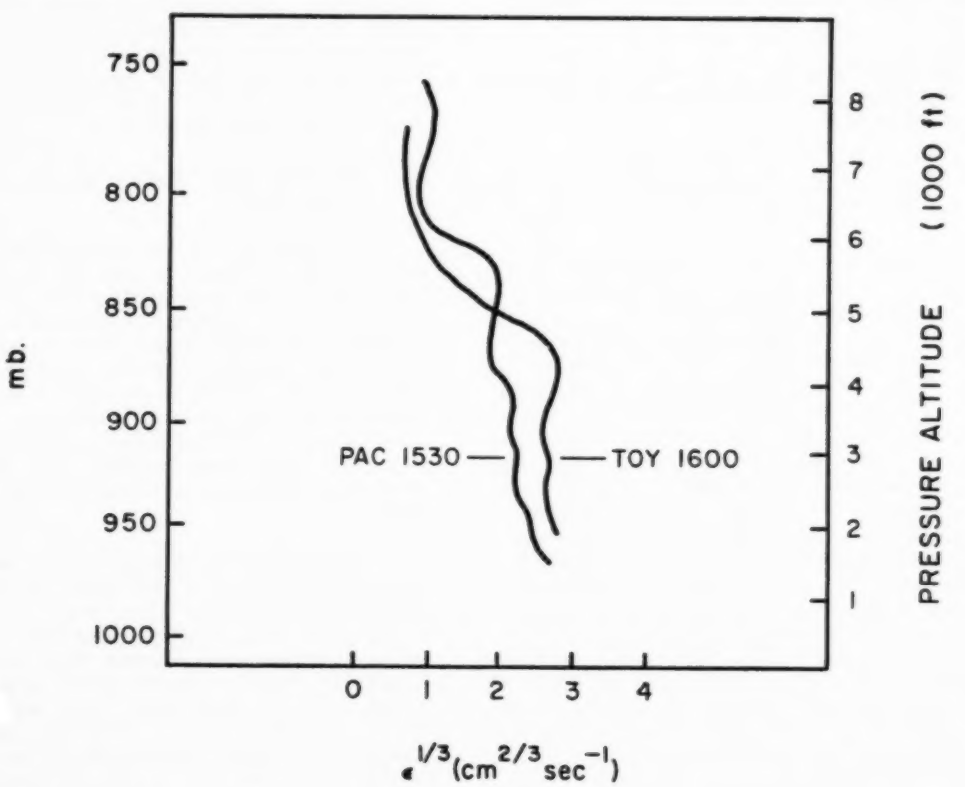

Figure 5.26. Plot of $\varepsilon^{1/3}$ vs. height indicated by the aircraft turbulence meter over PAC and TOY on 13 August 1971.

forces, the second (wind-shear) term in Equation 5.12 may be neglected giving:

$$\varepsilon = \frac{gH}{C_p \rho T} . \qquad (5.13)$$

Now, in the case of free convection (the state of the atmosphere where the vertical transfer of heat and momentum by mechanical turbulence can be neglected compared to that by heat convection), ε will tend to become almost independent of height) Lumley and Panofsky, 1964; Lenschow, 1970; Taylor, 1972).

However, returning to Figure 5.26, it can be seen that, proceeding upward from the surface, the magnitude of $\varepsilon^{1/3}$ is nearly constant with height over both TOY and PAC, but commences a decreasing trend about 1500 ft lower over TOY than PAC. Recalling Figure 5.25, it is apparent that this gradient of $\varepsilon^{1/3}$ over TOY coincides with the region of elevated heating observed at TOY; i.e., the region of elevated heating due to suspected elevated entrainment and/or aerosol warming. If either of these processes is associated with the gradient of $\varepsilon^{1/3}$ in the region of elevated heating, their contribution may possibly be ascertained in an examination of the dependency of Equation 5.13 with height (z).

Consider Equation 5.14 which is Equation 5.13 subsequent to differentiation with respect to height,

$$\frac{d\varepsilon}{dz} = \frac{g}{C_p \rho} \left[\frac{T \frac{dH}{dz} - H \frac{dT}{dz}}{T^2} \right] \qquad (5.14)$$

where g and ρ are assumed constant over the shallow layer (~30 mb) on which Equation 5.14 is operating. From Figure 5.25, it is seen that $T > 0$ and $\frac{dT}{dz} \leq 0$ over the region considered (830-800 mb). Also, H must be greater than zero in order for ε in Equation 5.13 to be positive (Figure 5.26 shows that $\varepsilon > 0$). Since g, C_p, and ρ are all positive, it is clear that $\frac{dH}{dz} < 0$ in order for $\frac{d\varepsilon}{dz} < 0$, as is the case in the 830-800 mb region over TOY in Figure 5.26. Then, a downward flux of heat in this region due to the elevated entrainment process would result in $\frac{dH}{dz} < 0$ in Equation 5.14, and support the observed gradient of $\frac{d\varepsilon}{dz}$. As a consequence of this discussion, it is strongly implied that the "skewed hour glass" elevated heating profile observed at ARC-TOY (Figure 5.25) was related to the elevated entrainment process, and that this resulted in a decrease of the mixing layer depth and subsequent inhibition to convective cloud activity.

Even though the spatial location of convective cloud activity on 13 August 1971 was at the opposite end of the metropolitan area when compared to the location on 23 August 1971, it is apparent that the factors governing the spatial distribution on both days are consistent throughout the analyses. As in the case study of 23 August 1971, it seems that the 13 August 1971 mixing layer depth and spatial distribution of convective cloud activity in the St. Louis area are directly related to aerosol structure and the modification of vertical temperature profiles.

5.4 9 August 1971 Case Study

It appears that after sorting out the effect of a broader scale advective process, 9 August 1971 was a day where urban area influences may have induced the spatial modification of vertical temperature structures. Aitken nucleus samples collected with the airborne Gardner counter through the vertical over PAC suggested that a denser aerosol layer existed over that vicinity as compared with ARC. The formation of an elevated stable layer at PAC by 0700 (while none existed at ARC), and subsequent warming below this layer served to shrink the potential mixing layer depth at PAC, inhibiting convective cloud activity at that location. Therefore, an elevated stable layer may have had a causal effect on the modification of vertical temperature structure which resulted in spatially separated regions of stimulation and inhibition to convective cloud activity.

5.5 Moisture Distribution on the Three Case Study Days

Although water vapor distributions were frequently mentioned in the developmental analyses of the case studies, no specific conclusions regarding the generation or transport of water vapor were presented. Due to the available data, it was felt that this subject should be relagated a cursory priority in the research approach. However, some general considerations, applicable to all three days investigated, will now be presented without reference to individual data.

Inspection of morning (0700) soundings showed no conclusive spatially preferential regions of increased water vapor; however, on certain days, one area may show a slightly greater water vapor content than another. Generally, both urban and rural areas showed a reduction in mean water vapor content in the mixing layer from 0700-1230; however, surface dew point temperature often increased in this time period. Early afternoon was generally the preferred time for the occurrence of primary convective activity, and aircraft soundings recorded in these regions

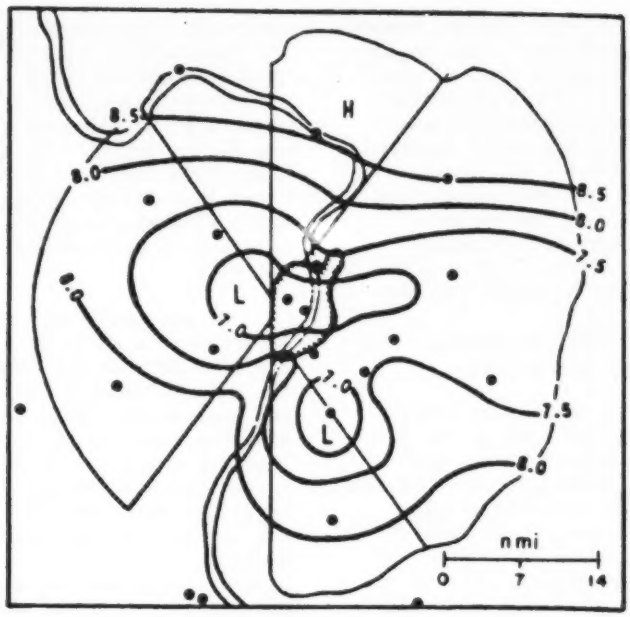

Figure 5.27. "Dry" summer rainfall (inches) for the St. Louis area during the period 1949-1968 (after Huff et al., 1971).

(usually outside the area of major urban buildup) showed a significant increase in moisture in the layer below cloud base. The early afternoon increase in moisture was usually associated with the deepening of the surface convection (mixing) layer; and in accordance with the observed increasing surface dew point temperature, this moisture influx appeared to have a low-level origin which was progressively distributed upward through the vertical.

These observations suggest that two mechanisms may be operating in the urban-rural complex. First, a mechanism where relatively drier air is injected into the upper portion of the mixing layer, and is noticeable through the morning hours. Secondly, a mechanism where low-level water vapor is being generated near the surface (or advected along the surface), and is distributed upward through the mixing layer, making its effect detectable in the early afternoon period.

5.6 Climatological Implications

As previously mentioned in the Introduction of this paper, Beebe and Morgan (1972) have associated the St. Louis precipitation anomaly with summer, convective, daytime, air mass rain storms. In addition they have found that the anomaly occurred with a deep mixing layer. These synoptic conditions were met on the three case study days, and results from our analyses compliment their findings.

The spatial distribution of precipitation in the St. Louis area for dry summers, as analyzed by Huff et al. (1971), is shown in Figure 5.27. Recall from Section 1.3 that August 1971 certainly qualified as a dry summer. The results from analysis of our case studies of 23, 13 and 9 August 1971, supported by the climatological inferences of Huff et al.(1971) and Huff and Changnon (1972), seem to indicate that under the "dry" synoptic regime of these case studies, the immediate area of major urban buildup may not be a region of precipitation stimulation, and may actually serve to inhibit the precipitation process at that location. When considered over a climatologically significant period, it is suggested that the presence of elevated aerosol layers and the entrainment mechanism associated with elevated stable layer inhibit convective cloud activity. Since aerosol layers and elevated stable layers are more prevelant over the major urban area, they may selectively modify the spatial distribution of convective cloud activity for dry summers along the lines proposed in this work.

VI. SUMMARY AND CONCLUSIONS

6.1 General Considerations

The three case study days examined were all subjected to the influence of a similar

synoptic regime; i.e., a high pressure summer air mass, light wind situation. This regime proved fortuitous in the sense that it provided a field laboratory which facilitated the study of urban area convective cloud activity virtually uncomplicated by external meteorological disturbances. As a consequence, the results of this work should not be directly applied to synoptic regimes characterized by large external forcing functions (e.g., squall lines, high wind) without due consideration of these factors.

6.2 Regions of Preferential Convective Activity in the St. Louis Area

Analyses of data on three case study days showed that regions existed in the St. Louis area where convective activity was favorable, while simultaneously, other regions existed where convective activity was inhibited. On two of the case study days (9 and 23 August 1971), the primary convective activity was located immediately east of the St. Louis metropolitan area, and on the remaining case study day (13 August 1971), the primary convective activity was centered west of the metropolitan area. On 9 and 23 August 1971 towering cumulus which emitted precipitation developed in a preferential convective region while the formation of substantial cumulus was inhibited over and to the west of the metropolitan area. On 13 August 1971, cumulus clouds started to develop over the St. Louis area with a relatively uniform spatial distribution, but were then selectively inhibited over and to the east of the metropolitan area while towering cumulus developed to its west.

Investigation of meteorological data showed that this spatially selective distribution of convective cloud activity was chiefly a function of a differential in vertical temperature structures and mixing layer depth through the urban-rural area. The influence of synoptic factors (e.g., advection from outside the St. Louis area) were considered and determined to be incapable of producing this anomaly without an urban meso-scale interaction. It is concluded that the St. Louis urban area played a salient role in the modification of vertical temperature structure and mixing layer depth; and that this modification was the chief contributor to the spatially preferential regions of convective activity.

6.3 Urban Influences on Vertical Temperature Structure

The case study data showed that the presence of an elevated thermally stable layer was the major inhibitor of convective activity; cloud formation was favored where the temperature lapse rate was dry adiabatic in a deep mixing layer which extended from the surface to cloud base, and there was an absence of an elevated stable layer capping the mixing layer. In addition, two of the case study days (9 and 23 August 1971) exhibited significant (2-3K) heat islands vertically through the mixing layer beneath the location of preferential convective cloud activity.

It was found that elevated stable layers were a characteristic feature of both the 0700 ARC and 0700 PAC soundings during the month of August 1971, but that they did not necessarily occur simultaneously or display the same intensity. It is suggested that the character of an early morning elevated stable layer may be a contributory factor in the subsequent formation of vertical temperature structures as the day progressed. The aerosol distribution associated with an early morning elevated stable layer appears to produce an asymmetrical heating profile through the vertical when subjected to solar insolation, where a significant portion of the heating in this air column is distributed in the vicinity of the stable layer. This heating profile was likened to a "skewed hour glass" and was found to be typical of regions where convective activity was inhibited. The net observed result of this elevated heating process is then the development of a thermally stable layer which caps the mixing layer and shrinks its potential depth. The stable layer may eradicate in time if sufficient surface heating is supplied, but has the initial effect of inhibiting convective cloud formation. Since elevated stable layers and the associated asymmetrical heating were spatially selective processes, they were considered to be a function of the urban environment and an examination of possible contributory mechanisms was considered.

6.4 Mechanisms Associated with the Formation of Elevated Stable Layers and Elevated Heating

A process whereby the air in the vicinity of an elevated stable layer may be warmed was derived from a fluids experiment conducted by Rouse and Dodu (1955). The experiment showed that non-turbulent mass may be entrained through a sharp density discontinuity into a turbulent layer. This may be considered analogous to an atmospheric system where the turbulent layer is a thermal mixing (convection) layer, separated from the non-turbulent region above by an elevated stable layer. A dimensional analysis comparison of the fluid and atmospheric parameters suggested

that this entrainment process is feasible in the atmosphere. A discussion of the entrainment of a non-turbulent field by an adjacent turbulent region (Townsend, 1956) helped to elucidate the model. Theoretical investigations (Ball, 1960; Lilly, 1968), laboratory experiments (Deardorff et al., 1969; Fanaki, 1971) and other aircraft supported field studies (Lenschow and Johnson, 1968; Lenschow, 1970, 1973) have lent credence to the model and suggested that the magnitude of the entrainment process is contingent on the underlying surface and meteorological conditions. During Project METROMEX, early morning elevated turbulence recorded by the aircraft in the vicinity of an elevated aerosol layer, as well as thermal turbulence generated from surface heating in the mixing layer, was suggested as a possible forcing mechanism which could facilitate the entrainment process and observed elevated heating. The early morning elevated turbulence, provided a localized source of turbulent kinetic energy at the base of the elevated stable layer, may induce a more effective result than elevated entrainment stimulated by surface heating.

The work of Atwater (1970) has suggested a mechanism where radiative cooling of an aerosol layer is capable of producing an elevated stable layer at the top of the aerosol layer. Available lidar data from the SRI/EPA Mark VIII lidar unit during the month of August 1971 has shown that early morning elevated stable layers were characteristically located at the top of an aerosol layer. In the one case when the lidar unit was operated through the nocturnal hours, an elevated stable layer was detected on the morning sounding capping an elevated aerosol which was the residue of the previous day's mixing (convection) layer. Atwater's numerical model predicts that the warming of an aerosol layer from solar insolation may reach significant magnitude and that the major portion of this warming would be found in the upper portion of the aerosol layer (the region below the elevated stable layer). The modification of vertical temperature structures as derived from data in this paper were found to be compatible with these considerations.

It was shown that both the entrainment and radiative heating processes may compatibly produce a region of elevated heating in the vicinity of an elevated stable layer which would effectively reduce the mixing layer depth and inhibit convective cloud activity. While the observed data does not conclusively prove, or disprove, either of these mechanisms, it is strongly implied that these mechanisms may be active, and that further research in these areas must be expanded.

ACKNOWLEDGMENTS

This research was made possible by the Environmental Protection Agency, Grant R-800875 to the Department of Atmospheric Resources, College of Engineering, University of Wyoming.

REFERENCES

Ackerman, B., 1971: Moisture content of city and country air. Proc. Conf. on Air Pollut. Meteor., Raleigh, North Carolina, 154-157.

American Meteorological Society, 1968: Glossary of Terms Frequently Used in Air Pollution. American Meteorological Society, Boston, Massachusetts, 34 pp.

Anderson, G. E., 1971: Mesoscale influence on wind fields. J. Appl. Meteor., 10(3), 377-386.

Angell, J. K., D. H. Pack, W. A. Hass and W. H. Hoecker, 1968: Tetroon flights over New York City. Weather, 23(6), 194-204.

Arnold, G. R., 1964: Local Inversion, Air Currents and Smoke Pollution in the Cahokia Bottom. Ph.D. Dissertation, Sever Institute of Technology, Washington University, St. Louis, Missouri, 192 pp.

Atkinson, B. W., 1968: A preliminary investigation of the possible effect of London's urban area on the distribution of thunder rainfall, 1951-1960. Trans. Inst. Brit. Geogr., 44, 97-118.

_____, 1969: A further examination of the urban maximum of thunder rainfall in London, 1951-1960. Trans. Inst. Brit. Geogr., 48, 97-120.

_____, 1970: The reality of the urban effect on precipitation -- a case study approach. W. M. O. Symp. on Urban Climates and Building Climatology, Tech. Note No. 108, Brussels, Belgium, 342-360.

_____, 1971: The effect of an urban area on the precipitation from a moving thunderstorm. J. Appl. Meteor., 10(1), 47-55.

Atwater, M. A., 1970: Investigation of the radiation balance for polluted layers of the urban environment. Ph.D. Dissertation, Department of Meteorology and Oceanography, New York University, New York, New York, 141 pp.

Ball, F. K., 1960: Control of inversion height by surface heating. Quart. J. Roy. Meteor. Soc., 86(370), 483-494.

Baynton, H. W., 1968: Stability inferences from precision rawins. Mon. Wea. Rev., 96(1), 47-53.

Beebe, R. C. and G. M. Morgan, Jr., 1972: Synoptic analysis of summer rainfall periods exhibiting urban effects. Preprints of the Conf. on Urban Environ. and Second Conf. on Biometeor., Philadelphia, Pennsylvania, 173-176.

Bellamy, J. C., 1949: Objective calculations of divergence, vertical velocity and vorticity. Bull. Amer. Meteor. Soc., 30(2), 45-49.

Black, J. F., 1962: Weather control: Use of asphalt coatings to tap solar energy. Science, 139(3569), 226-227.

Bornstein, R. D., 1968: Observations of the urban heat island effect in New York City. J. Appl. Meteor., 7(4), 575-582.

_____, A. Lorenzen and D. S. Johnson, 1972: Recent observations of urban effects on winds and temperatures in and around New York City. Preprints of the Conf. on Urban Environ. and Second Conf. on Biometeor., Philadelphia, Pennsylvania, 28-33.

Buckingham, E., 1915: Model experiments and the form of empirical equations. Trans. ASME, 37, 263-296.

Busch, N. and H. A. Panofsky, 1968: Recent spectra of atmospheric turbulence, 1968. Quart. J. Roy. Meteor. Soc., 94(400), 132-148.

Cermak, J. E., V. A. Sandborn, E. J. Plate, G. H. Binder, H. Chuang, R. N. Meroney and S. Ito, 1966: Simulation of atmospheric motion by wind-tunnel flows. Tech. Report. CER 66 JEC-VAS-EJP-GHB-HC-RMN-SI 117, Fluid Dynamics and Diffusion Laboratory, Colorado State University, Fort Collins, Colorado, 101 pp.

Chandler, T. J., 1962: Temperature and humidity traverses across London. Weather, 17(7), 235-241.

_____, 1965: The Climate of London. Hutchison & Co., London, 292 pp.

_____ 1966: London's heat island. Biometeorology II, Pergamon Press, London.

_____ 1967: Absolute and relative humidity in towns. Bull. Amer. Meteor. Soc., 48(6), 394-399.

Changnon, S. A., Jr., 1971: 1971 Operational Report for METROMEX. Illinois State Water Survey, Urbana, Illinois, 93 pp.

Charlson, R. J. and M. J. Pilat, 1969: Climate: The influence of aerosols. J. Appl. Meteor., 8(6), 1001-1002.

_____ and _____, 1971: Reply. J. Appl. Meteor., 10(4), 841-842.

Clarke, J. F., 1969: Nocturnal urban boundary layer over Cincinnati, Ohio. Mon. Wea. Rev., 97(8), 582-589.

Daily, J. W. and D. R. F. Harleman, 1966: Fluid Dynamics. Addison-Wesley, Reading, Massachusetts, 454 pp.

Davidson, B., 1967: A summary of the New York urban air pollution dynamics research program. J. Air Pollut. Contr. Assoc., 17(3), 154-158.

Davis, P. A., 1965: The application of infrared flux models to atmospheric data. J. Appl. Meteor., 4(2), 263-271.

Deardorff, J. W., G. E. Willis and D. K. Lilly, 1969: Laboratory investigation of non-steady penetrative convection. J. Fluid Mech., 35(1), 7-31.

De Marrais, G. A., 1961: Vertical temperature difference observed over an urban area. Bull. Amer. Meteor. Soc., 42(8), 548-554.

Duckworth, F. A. and J. S. Sandberg, 1954: The effect of cities upon horizontal and vertical temperature gradients. Bull. Amer. Meteor. Soc., 35(5), 198-207.

Fanaki, F. H., 1971: A simulation of heat flow in the lower troposphere by a laboratory model. Boundary-Layer Meteor., 1(3), 345-367.

Georgii, H. W., 1968: The effects of air pollution on urban climates. W. M. O. Symp. on Climates and Building Climatology, Tech. Note No. 108, Brussels, Belgium, 214-237.

Hanna, S. R., 1968: A method of investigating vertical eddy transport in the planetary boundary layer using characteristics of the vertical velocity spectrum. J. Atmos. Sci., 25(6), 1026-1033.

Hass, W. A., W. H. Hoecker, D. H. Pack and J. K. Angell, 1967: Analysis of low-level, constant volume balloon (tetroon) flights over New York City. Quart. J. Roy. Meteor. Soc., 93(398), 483-493.

Hidy, G. M., 1967: Adventures in atmospheric simulation. Bull. Amer. Meteor. Soc., 48(3), 143-161.

Hoddinott, M. H. O., 1960: Funnel cloud at Chester, July 28, 1959. Meteor. Mag., 89(1053), 124-125.

Huff, F. A. and S. A. Changnon, Jr., 1972: Climatological assessment of urban effects of precipitation. Final Report - Part II. Description of Individual Urban Studies, Illinois State Water Survey, Urbana, Illinois, 237 pp.

_____, _____ and T. A. Lewis, 1971: Climatological assessment of urban effects on precipitation. Preprints of the Conf. on Air Pollut. Meteor. of the Amer. Meteor. Soc., Raleigh, N. C., 98-103.

Kratzer, P., 1956: Das Stadklima. Second Edition, Trans. by Amer. Meteor. Soc., Boston, Massachusetts, 221 pp.

Landsberg, H. E., 1956: The climate of towns. In Man's Role in Changing the Face of the Earth. University of Chicago Press, Chicago, Illinois, 584-606.

_____, 1962: Physical Climatology. Second Edition, Third Printing, Gray Printing Co., Du Bois, Pennsylvania, 446 pp.

_____, 1970: Man-made climatic changes. Science, 170(3964), 1265-1274.

Lenhard, R. W., 1970: Accuracy of radiosonde temperature and pressure-height determination. Bull. Amer. Meteor. Soc., 51(9), 842-847.

Lenschow, D. H., 1970: Airplane measurements of planetary boundary layer structure. J. Appl. Meteor., 9(6), 874-884.

_____, 1973: Two airplanes of planetary boundary layer modification over the Great Lakes. Accepted for publication in J. Appl Meteor.

_____ and W. B. Johnson, 1968: Concurrent airplane and balloon measurements of atmosphere boundary-layer structure over a forest. J. Appl. Meteor., 7(1), 79-89.

Lilly, D. K., 1968: Models of cloud-topped mixed layers under a strong inversion. Quart. J. Roy. Meteor. Soc., 94(400), 292-309.

Ludwig, F. L., 1968: Urban temperature fields. W. M. O. Symp. on Urban Climates and Building Climatology, Tech. Note No. 108, Brussels, Belgium, 80-107.

Lumley, J. L. and H. A. Panofsky, 1964: The structure of atmospheric turbulence. Interscience Publishers, New York, New York, 329 pp.

MacCready, P. B., Jr., 1970: An application memorandum for the MRI Universal Indicated Turbulence System (UITS). Meteorology Research Incorporated, Altadena, California, 17 pp.

Malkus, W. V. R., 1954: Discrete transitions in turbulent convection. Proc. Roy. Soc., A225, p. 196.

_____, 1955: The effects of a large island upon the trade-wind air stream. Quart J. Roy. Meteor. Soc., 81(350), 538-550.

_____, 1957: Trade cumulus cloud groups: Some observations suggesting a mechanism of their origin. Tellus, 9(2), 33-44.

McCormick, R. A. and J. A. Ludwig, 1967: Climate modification by atmospheric aerosols. Science, 156(3780), 1358-1359.

Mitchell, J. M., 1961: The temperature of cities. Weatherwise, 14(6), 224-229.

_____, 1970: The effect of atmospheric aerosols on climate with special reference to surface temperature. NOAA Tech. Memo. EDS 18, 28 pp.

Morrissey, J. F. and F. J. Brousaides, 1970: Temperature induced errors in the M-476 humidity data. J. Appl. Meteor., 9(5), 805-808.

Munn, R. E. and I. M. Stewart, 1967: The use of meteorological towers in urban air pollution programs. J. Air Pollut. Cont. Assoc., 17(2), 98-101.

_____, M. S. Hirt and B. F. Findlay, 1969: A climatological study of the urban temperature anomaly in the lakeshore environment at Toronto. J. Appl Meteor., 8(3), 411-422.

Oke, T. R. and F. G. Hannell, 1968: The form of the urban heat island in Hamilton, Canada. W. M. O. Symp. on Urban Climates and Building Climatology, Tech. Note No. 108, Brussels, Belgium, 113.

Okita, T., 1960: Estimation of direction of airflow from observations of rime ice. J. Meteor. Soc. Japan, 38, 207-209.

Olsson, L. E., W. L. Tuft, W. P. Elliott and M. P. McCormick, 1971: Observational study of the haze (mixing) layer in Western Oregon using laser radar, instrumented aircraft and meteorological balloons. Paper presented at the 64th Air Pollut. Control Assoc. Annual Meeting, Atlantic City, New Jersey, 13 pp.

Pooler, F., 1963: Airflow over a city in terrain of moderate relief. J. Appl. Meteor., 2(4), 446-456.

Rouse, H., 1950: Engineering Hydraulics. Wiley and Sons, New York, New York, 92 pp.

_____ and J. Dodu, 1955: Diffusion turbulence á travers une discontinuité de densité. La Houille Blanche, No. 4, 522-529.

Sasakura, K., 1965: On the distributions of relative humidity in Tokyo and its secular change in the heart of Tokyo. Tokyo J. of Climatology, 2, p. 45.

Saucier, W. J., 1955: Principles of Meteorological Analyses, University of Chicago Press, Chicago, Illinois, 438 pp.

Schmidt, F. H., 1963: Local circulation around an urban area. Inter. J. Air Water Pollut., 7, 925-926.

Schneider, S. H., 1971: A comment on "Climate: The influence of aerosols". J. Appl. Meteor. 10(4), 840-841.

Sheppard, P. A., 1952: Discussion of paper by Taylor (1952). Quart J. Roy. Meteor. Soc., 78(338), 647-648.

Spangler, T. C., 1972: Dynamically induced meso-scale variations of the urban mixing layer depth, M. S. Thesis, Department of Atmospheric Resources, University of Wyoming, Laramie, Wyoming, 94 pp.

Stout, G. E., 1962: Cloud initiation in industrial areas. Proc. of Symp. of Air over Cities, Cincinnati, Ohio, 147-153.

Summers, P. W., 1965: An urban heat island model -- its role in air pollution problems, with application to Montreal. Paper presented at the First Canadian Conf. on Micrometeorology, Toronto, Ontario, Canada, 22 pp.

Sundborg, A., 1950: Local climatological studies of the temperature conditions in an urban area. Tellus, 2(3), 222-232.

Taylor, R. J., 1952: The dissipation of kinetic energy in the lowest layers of the atmosphere. Quart. J. Roy. Meteor. Soc., 78(335), 179-185.

_____, 1972: Aircraft measurements of dissipation of turbulent kinetic energy. Quart J. Roy. Meteor. Soc., 98(417), 658-661.

Thomas, D. B. and A. A. Townsend, 1957: Turbulent convection over a heated horizontal surface. J. Fluid Mech., 2, 73.

Townsend, A., 1956: The Structure of Turbulent Shear Flow. Cambridge University Press, Cambridge, England, 315 pp.

U. S. Air Force, Air Weather Service, 1955: Accuracies of radiosonde data. AWS Tech. Rep. 105-133, 12 pp.

Uthe, E. E. and J. H. S. Kealoha, 1972: Lidar observations of aerosol structure over St. Louis, Missouri, during METROMEX 1971. Final Technical Report, Stanford Research Institute, Menlo Park, California, 44 pp.

Warner, J. and J. W. Telford, 1967: Convection below cloud base. J. Atmos. Sci., 24(4), 374-382.

Webb, E. K., 1958: Vanishing potential temperature gradient in strong convection. Quart J. Roy. Meteor. Soc., 84(359), 119-125.

Weurch, D. E., 1971: An investigation of the resultant transport wind within the urban complex. NOAA Tech. Memorandum NWS CR-44, 19 pp.

Woolum, C. A. and N. L. Canfield, 1968: Washington metropolitan area precipitation and temperature patterns. ESSA Tech. Memorandum WBTM-ER-28, 32 pp.

APPENDIX A. Instrumentation in the University of Wyoming mobile unit.

Function	Device	Range	System Resolution	System Accuracy
Temperature*	Rosemount 104C platinum resistance sensor - ventilated	-50 to +50C	0.1C	±0.2C
Dew Point*	Cambridge Systems Model 880	-40 to +50C	0.3C	±2.0C
Wind speed*	RAIM No. 436 anemometer	1 to 100 mph	2 mph	±5%
Wind direction*	RAIM No. 437 vane	-	16 point	-
Wind sounding	Single theodolite	-	-	-
Atmospheric Pressure	Belfort Model 355 R remote microbarograph	650 to 1050 mb	0.5 mb	Depends on reference
Air filter samples for ice nuclei measurements*	3 x 3 sequential sampler with difference pressure transducer	20 lit min^{-1} per filter	-	±5% of volume sampled
Rain drop-size distribution**	Rd-60 momentum sensor	0.3 > D > 10 mm	20 size groups	±5%
Rate of rainfall*	Stand-tube with discharge nozzle	5 > R > 50 mm hr^{-1} steady, and R = 200 mm hr^{-1} transient	3 mm hr^{-1}	±5 mm hr^{-1} at high R

*Parameters recorded on multipoint strip chart recorder.

**Parameters recorded on analog magnetic tape.

Reproduced from best available copy.

APPENDIX B. Instrumentation on the University of Wyoming aircraft.

Parameter Measure	Manufacturer and Model Number	Range	Accuracy Sensor / System	Resolution
Temperature	Rosemount Engr. Model 102 de-iced	-50C to +50C	±1C / ±0.1C	0.1C
Dew Point	Cambridge Systems Model 137-C3	-50C to +50C	±0.5C above 0C / ±0.1C ±1.0C below 0C	0.1C
Heading	King Radio Model KP1550A	360°	±2° of local magnetic heading /1°	1°
VOR Azimuth	King Radio Model KNR-660	360°	±2° / ±1°	1°
DME	King Radio Model KDM-700	0 to 9 mm	±0.1 nm or ±0.2% or range Whichever is greater / ±0.1 nm	0.1 nm
Altitude	Ball Model 210B Total pressure Transducer	0 to 25 Kft	0.05% / 0.1%	continuous
IAS	Rosemount Model 1301D Differential Pressure Transducer	0 to 250 Kts	±2 Kts / ±1 Kts	1 K
Manifold Pressure	Computer Instruments	15 to 30" Hg	5% / ±0.1%	0.1" Hg
Vane angle or angle of Attack	U. W. Atmospheric Research Group	99°	2% / 2%	0.1°
Pitch Angle	Smith Industries Lmtd-Aviation Division Model 402RGS/-2	0 to ±20°/sec	2% / 2%	0.04° sec^{-1}
Roll Angle	Smith Industries Lmtd-Aviation Division Model 402RGS/-2	0 to ±20°/sec	2% / 2%	0.04° sec^{-1}
Vertical Acceleration	United Controls Model No. 2152	±3 g's	1% of full range	0.006 g's
Liquid Water	Johnson Williams Model No. LWH	0 to 3 gm m^3	unknown / ±0.1 g m^{-3}	0.1 g m^{-3}
Turbulence ($\varepsilon^{1/3}$)	M. R. I.	Inertial Sub-range = 10^{-1} to 5 x 10^2 m $0 \leq \varepsilon^{1/3} \leq 10$	-	0.01 $cm^{2/3}$ sec^{-1}
Ice Nuclei	Membrane Filters			
Aitken Particles	Gardner Counter	10^2-10^7 particles/cc	-	-